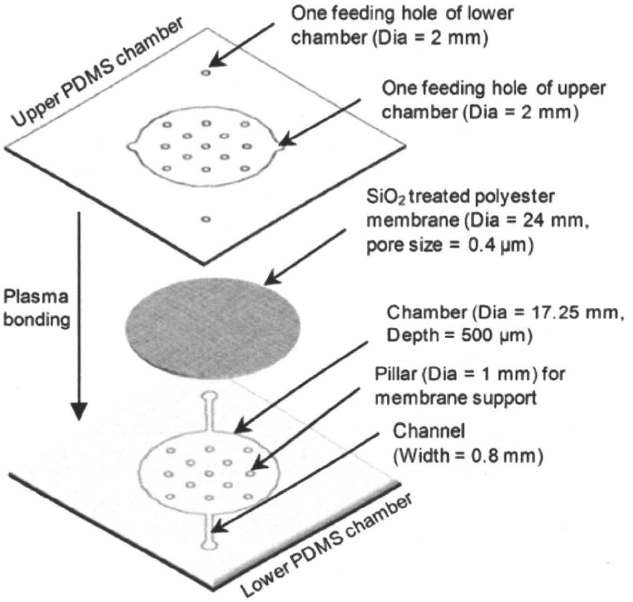

Fig. 1 Details of the PDMS chambers and membrane used to fabricate the MB. The membrane is sandwiched between the two PDMS chambers using the common O_2 plasma method. Both top and bottom PDMS chambers have two feeding holes to inject cells and exchange culture medium. Cells are cultured only on the top face of membrane

2.2 Fabrication of the MB

Details of the MB fabrication method are presented elsewhere (Kimura et al. 2008). Briefly, negative photoresist SU-8 2100 (Microchem Co.) was used to create the mold masters with the desired pattern. Then PDMS polymer (Silpot 184; Dow Corning Corp.) was mixed with its curing agent at a 10:1 ratio, poured over the mold masters, cured for 2 h at 75°C and peeled off thereafter.

The polyester membranes (pore size 0.4 μm, thickness 10 μm) were removed from Transwell Inserts 3450 (Corning Inc.). To bond the membrane with the PDMS layers, both sides of the membrane were coated with a thin layer of SiO_2 by sputtering for 20 s at 150 W and 0.5 Pa. The membrane was sandwiched between the two PDMS chambers following O_2 plasma treatment. Flow chips were then attached to the silicon tubing for connecting syringes; medium and reagents were manually introduced using those syringes.

2.3 Pre-treatment of experimental group (6-WP, TW and MB)

Because SiO_2 was used to coat the polyester membrane incorporated in the MB, the top side of the TW membrane was also coated with SiO_2 by sputtering. The TW and MB were then sterilized for 2 h under UV light. A 0.2% w/v gelatin solution was applied to cover the surface of the 6-WP and the membrane surfaces of the TW and MB, which was followed by 6 h of incubation. Culture medium for the experimental group was added to these culture systems for pre-incubation before seeding mESCs.

2.4 Routine cell culture

mESCs were routinely cultured in 60 mm gelatin coated dishes (Iwaki). Cell inoculation density was 2×10^4 cells/cm^2, and the cells were passaged every other day. Culture medium composition for routine culture was high glucose DMEM (DMEM; Gibco) containing 20% ESC qualified Fetal Bovine Serum (FBS; Gibco), 1000 U/ml ESGRO-LIF (Chemicon), 1% MEM non-essential amino acids (Gibco), 2 mM GlutaMax-I (Gibco), 100 U/ml penicillin, 100 U/ml streptomycin (Gibco) and 0.1 mM 2-mercaptoethanol (Gibco). The cells were maintained in a 37°C humidified environment containing 5% CO_2.

2.5 Cell culture in the experimental group

mESCs in the experimental group were cultured using the same medium as for routine culture except that DMEM and FBS were replaced with Knockout DMEM (Gibco) and 15% Knockout Serum (KSR; Gibco), respectively. KSR was used because it contains fewer extrinsic proteins. For the experimental group, cell inoculation density was 2×10^4 cells/cm^2. Cell culture in the experimental group was continued for 5 days. Culture medium of the 6-WP, the lower chambers of the TW and MB were changed daily. The upper chamber culture medium of the TW and MB were not changed. Morphological examination of the cells under microscope was performed daily. For inhibition experiments, Fibroblast Growth Factor Receptor (FGFR) antagonist SU5402 (Mohammadi 1997) (Calbiochem) at 10 μM and BMP4 antagonist Noggin (Smith and Harland 1992) (R&D Systems) at 100 ng/ml were added to the culture medium.

2.6 Glucose concentration measurement

Culture medium from the 6-WP, the lower chamber of the TW and MB were collected every day during the 5-day culture. On the 5th day, the culture medium from the upper chambers of the TW and MB were also collected. Glucose concentrations were measured with a glucose analyzer (GA05, A&T Corp., Japan).

2.7 Cell collection and qPCR analysis

Isolation of total mRNA was performed using Trizol Reagent (Invitrogen). In all culture systems, cells were dissociated using Trypsin (Gibco), counted and then lysed with Trizol. First-Strand cDNA Synthesis Kit (GE

Healthcare) was used to synthesize cDNA from the total mRNA. PCR reactions were carried out with a 7500 Real-Time PCR System (Applied Biosystems) using Quantitect SYBR Green PCR Kit (Qiagen). All steps were performed according to the manufacturers' instructions. Primers for cDNA amplification are listed in Table 1. qPCR were performed at least in duplicate. Raw data of PCR product amplification curves was analyzed using LinRegPCR v11.4 software (Ruijter et al. 2009) to determine the threshold cycles used in the $\Delta\Delta C_T$ method for relative quantification of gene expression. Geometric mean of the threshold cycles of reference genes GAPDH and β-Actin was used to normalize the target gene expressions. mESC culture at day 3 in the 6-WP was used as calibrator.

2.8 Statistical analysis

Student's *t*-test for comparing two groups and one way ANOVA with Tukey's post test for comparing more than two groups were performed for statistical evaluation using the demo version of GraphPad software (GraphPad Software, Inc.). Differences with a $P<0.05$ (*), $P<0.01$ (**), or $P<0.001$ (***) were considered to be statistically significant. All data are presented as the mean ± SEM.

3 Results

3.1 Effect of SiO_2 coating of the membranes on ESC behavior

SiO_2 coating on the membrane was necessary to bond it strongly with the PDMS layers, thereby preventing culture medium leakage in the MB. The coating did not affect permeability of the membranes as the measured glucose permeability of coated and non-coated membranes was the same (3×10^{-12} m^2s^{-1}). To examine whether the coating had any effect on cell behavior, we performed mESC culture on SiO_2-coated and non-coated membranes of the TW. Spread colonies of mESCs were observed on SiO_2-coated membranes (Fig. 2(a)), whereas these colonies remained spherical on the non-coated membranes (Fig. 2(b)). Cells attached weakly on the membranes without SiO_2 coating as the PBS wash during cell harvesting caused some cell loss. Consequently, the PBS wash was omitted for the non-coated membranes. However, no difference in cell growth was observed between SiO_2-coated and non-coated samples (fold changes in cell number relative to the seeded cells were 35.25±2.58 and 36.72±3.51, respectively). Furthermore, both of the cultures showed similar gene expression profile ($P>0.05$) (Fig. 3). Therefore, SiO_2 coating on the membrane was used for all the experiments.

3.2 Cell culture condition in the 6-WP, TW and MB

To keep the cellular microenvironment in the upper chamber of the MB and TW minimally disturbed, we only changed the culture medium of the lower chambers. Despite this, nutrients in these culture systems were sufficient as the glucose concentration throughout the 5 days of culture remained over half of the glucose concentration in fresh culture medium (0.02 M). Furthermore, no significant cell death was observed as assessed by the Trypan blue dye-exclusion test (data not shown) on day 5. Cell growth in all culture systems was similar ($P>0.05$) (Fig. 4). mESC culture in the TW and MB could be continued for more

Table 1 Genes and primers used in qPCR analyses

Genes	Description	Primer	Sequence (5′-3′)
GAPDH	Housekeeping gene	Forward	CAGAACATCATCCCTGCATC
		Reverse	CTGCTTCACCACCTTCTTGA
β-Actin	Housekeeping gene	Forward	TCACCCACACTGTGCCCATCTACGA
		Reverse	CAGCGGAACCGCTCATTGCCAATGG
Oct4	Pluripotency marker	Forward	AGAACCTTCAGGAGATATGC
		Reverse	TCTTCTCGTTGGGAATACTC
Sox2	Pluripotency marker	Forward	ACAAGGAAGGAGTTTATTCG
		Reverse	TTACCAACGATATCAACCTG
Rex1	Pluripotency marker	Forward	ACACAGAAGAAAGCAGGAT
		Reverse	GAACAATGCCTATGACTCAC
Nanog	Pluripotency marker	Forward	TGATTCTTCTACCAGTCCC
		Reverse	GGTCTTAACCTGCTTATAGC
FGF4	Cells' self-secreted soluble factor	Forward	TCGGTGTGCCTTTCTTTACC
		Reverse	ACCTTCATGGTAGGCGACAC
BMP4	Cells' self-secreted soluble factor	Forward	CCATCACGAAGAACATCTG
		Reverse	AATGTTTATACGGTGGAAGC

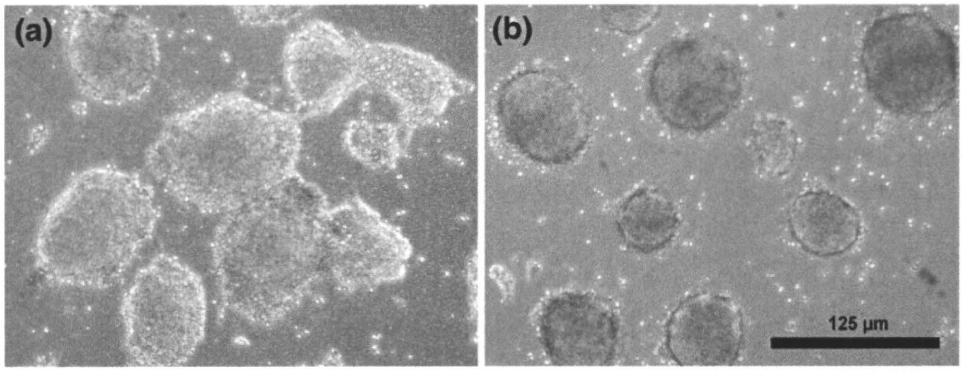

Fig. 2 mESC culture on day 5 on SiO_2-coated (**a**) or non-coated (**b**) polyester membranes of the TW. Cell colonies on the SiO_2-coated membrane are spread, whereas colonies on the non-coated membrane are round. Scale bar represents 125 μm

than 5 days, whereas cells began to die in the 6-WP after that period owing to nutrition depletion.

mESC colonies were extensively merged in the 6-WP (Fig. 5(a)) but they remained mostly as separated colonies in the TW and MB on day 5 (Fig. 5(b) and (c), respectively). Many differentiated cells showing a different morphology from usual mESCs were observed in the vicinity of cell colonies in the 6-WP and TW cultures (Fig. 5(d) and (e), respectively). In contrast, a few differentiated cells and smooth-bordered mESC colonies were observed in the MB (Fig. 5(f)), thereby indicating homogenous nature of the colonies.

3.3 Comparison of gene expression profiles among culture systems

In the MB culture, significantly higher expression levels of Oct4, Sox2 and Rex1 were observed compared to the 6-WP (Fig. 6). In addition, Sox2 and Rex1 expression in the MB were considerably higher than in the TW culture. These results showed that mESC pluripotency in the MB culture was higher than that in the macro-scale culture systems (6-WP and TW). Furthermore, both FGF4 and BMP4 were highly expressed in the MB culture compared to the TW (Fig. 6). However, only BMP4 expression in the MB was observed to be higher than in the 6-WP. Only Rex1 expression was different between the TW and 6-WP (Fig. 6).

3.4 Effects of soluble factors

To investigate whether dissimilarity in the activities of FGF4 and BMP4 between the MB and TW was responsible for the observed differences in the pluripotency markers expression (Sox2 and Rex1; Fig. 6), we performed inhibition experiments of FGF4 and BMP4 activities in the MB and TW cultures. FGF4 activity was inhibited using the small molecule SU5402, an antagonist of FGFR. This resulted in significantly increased expression of Nanog in the MB as well as TW cultures, but the other three pluripotency markers remained essentially unchanged (Fig. 7(a)). Expression of FGF4 increased, whereas that of BMP4 decreased in both MB and TW (Fig. 7(a)). We therefore concluded that the differentiation inducing activity of FGF4 suppressed Nanog expression, but did not affect the expression of Sox2 and Rex1 in the TW or MB. As a result, FGF4 cannot be

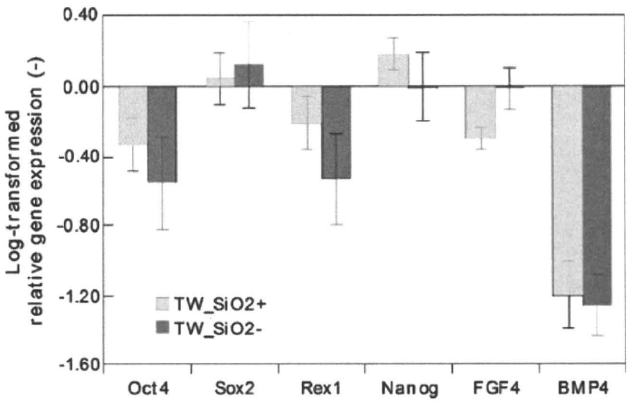

Fig. 3 Relative gene expression (Log_2-transformed) of mESCs cultured for 5 days on SiO_2-coated (TW_SiO2+) or non-coated (TW_SiO2−) membrane of the TW. Both cultures show similar gene expression profiles ($P>0.05$). Zero value represents the gene expression of mESC cultured in 6-WPs for 3 days. Columns and error bars represent mean ± SEM of three independent experiments

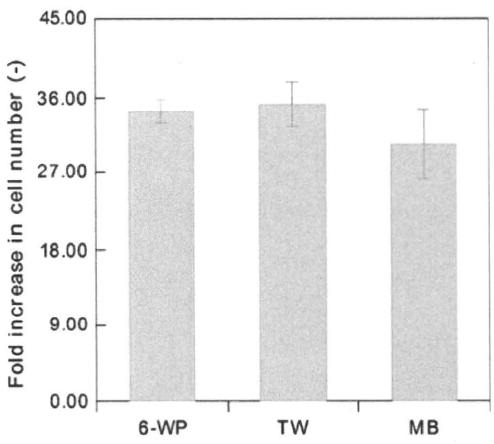

Fig. 4 Fold increase in cell number relative to the seeded cell number after 5 days of mESC culture in the 6-WP, TW and MB. Cell growths are similar in all culture systems ($P>0.05$). Columns and error bars represent mean ± SEM of four independent experiments

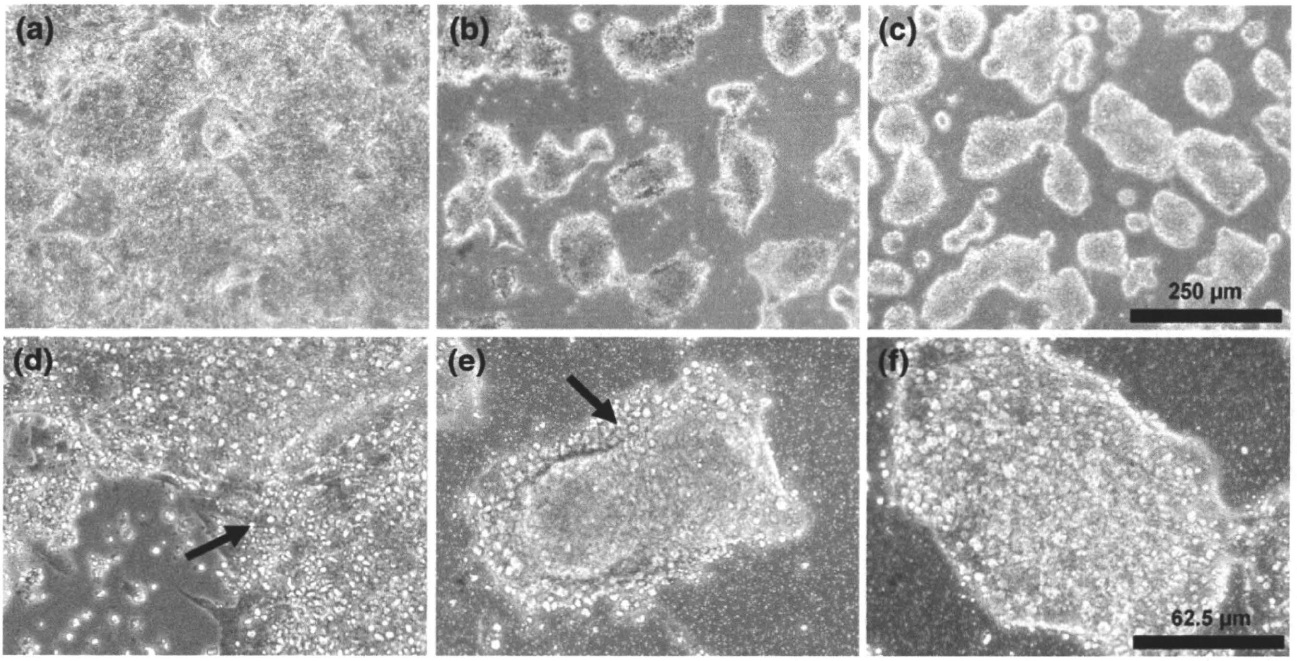

Fig. 5 mESC culture on day 5 in the 6-WP (**a**, **d**), TW (**b**, **e**) and MB (**c**, **f**). Arrows in the higher magnification images (**d**, **e**) indicate differentiated cells with a different morphology from the tightly packed colony type morphology of mESCs. Scale bars represents 250 μm (**a**, **b** and **c**), and 62.5 μm (**d**, **e** and **f**)

accounted for the differences in Sox2 and Rex1 expressions between the MB and TW cultures.

We then inhibited BMP4 activity using its antagonist Noggin. Expression of the pluripotency markers Sox2 and Rex1 decreased by the Noggin treatment in the MB, but they remained unchanged in the TW (Fig. 7(b)). In addition, both in the MB and TW culture, FGF4 and BMP4 expression remained unchanged by the same treatment. Sox2 and Rex1, which were upregulated more significantly in the MB as compared to the 6-WP and TW cultures (Fig. 6), decreased significantly by the Noggin treatment (Fig. 7(b)). Therefore, we can conclude that the activity of upregulated BMP4 (Fig. 6) is responsible for the better preservation of the mESC pluripotency in the MB.

4 Discussion

In this study, we developed a micro-scale culture system in which ESCs can be cultured in a diffusion dominant

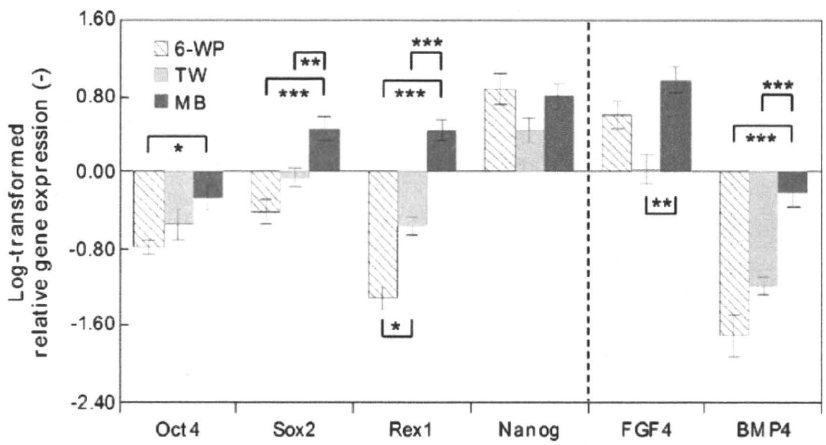

Fig. 6 Comparison of the gene expression profiles (Log_2-transformed) of mESCs cultured for 5 days in the 6-WP, TW and MB. Pluripotency markers (Oct4, Sox2 and Rex1) and soluble factors (FGF4 and BMP4) expression are upregulated in the MB. Zero represents gene expression of mESCs cultured in the 6-WP for 3 days. Columns and error bars represent mean ± SEM of six independent experiments. Statistical significance of the compared pairs are shown using the symbols *, ** and ***, representing *P*-values below 0.05, 0.01 and 0.001, respectively

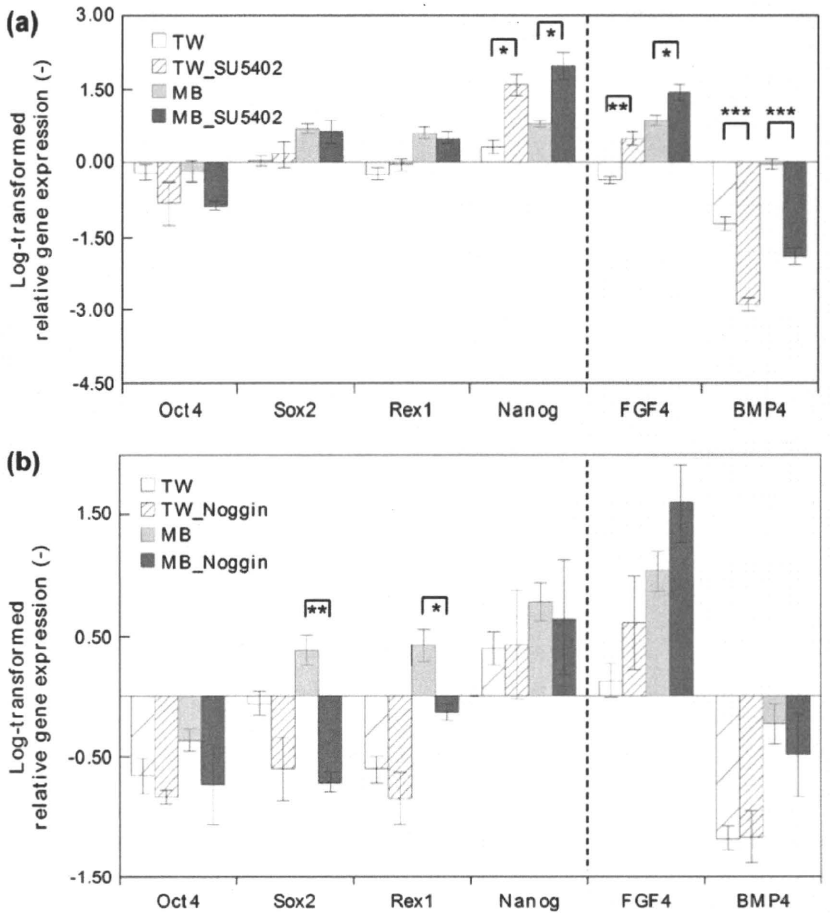

Fig. 7 Gene expression profiles (Log_2-transformed) of mESCs cultured for 5 days in the TW and MB, (**a**) with (TW_SU5402 and MB_SU5402) or without (TW and MB) inhibition of FGF4 signaling by SU5402; (**b**) with (TW_Noggin and MB_Noggin) or without (TW and MB) the BMP4 antagonist Noggin. Nanog expression both in the TW and MB increases following the SU5402 treatment. Sox2 and Rex1 expression decrease only in the MB following the Noggin treatment. Zero represents gene expression of mESCs cultured in 6-WP for 3 days. Columns and error bars represent mean ± SEM of four and three independent experiments for (a) and (b), respectively. Statistical significance of the compared pairs (TW against TW_SU5402; MB against MB_SU5402; TW against TW_Noggin; MB against MB_Noggin) are shown using symbols *, ** and ***, representing *P*-values below 0.05, 0.01 and 0.001, respectively

microenvironment without any limitation of nutrient supply for a long period of time. We observed better preservation of the mESC pluripotency in the micro-bioreactor than in the conventional macro-scale 6-WP and TW culture systems. We also demonstrated that autocrine effects of the up-regulated BMP4 cooperated with LIF to preserve the high pluripotency in the MB. Furthermore, the influence of FGF4 was similar in the TW and MB, whereas the influence of BMP4 was observed only in the MB.

A transcription network of Oct4, Sox2, Rex1 and Nanog maintains the pluripotency and proliferation of mESCs by suppressing the gene expression associated with differentiation (Masui et al. 2008; Niwa 2007). Usually, even in undifferentiated culture of mESCs in the presence of LIF, a proportion of the cells can undergo spontaneous differentiation (Smith 2001) which is associated with the decreased expression of those genes. Generally, overgrown differentiating mESC colonies have rough borders compared to the normal colonies. In the MB, mESC colonies were smooth-bordered, had few differentiated cells (Fig. 5(c) and (f)) and retained higher expression of the pluripotency markers (Fig. 6). These results indicated spontaneous differentiation of ESCs occurred less in the MB. Among the pluripotency markers, Sox2 and Rex1 showed prominently higher expression in the MB as compared to the WP and TW (Fig. 6). In fact, downregulation of Sox2 and Rex1 expression has a stronger correlation with loss of pluripotency of mESCs than the downregulation of Oct4 and Nanog expression (Palmqvist et al. 2005).

mESCs produce FGF4 extensively (Niwa et al. 2000) and BMP4 moderately (Johansson and Wiles 1995). FGF4 induces mESCs to differentiate (associated with the decreased expression of pluripotency markers of mESCs), which is counteracted by LIF and BMP4, as shown in Fig. 8 (Ying et al. 2008). In this study, although FGF4 was upregulated, high expression of BMP4 cooperated with LIF to preserve a high expression of pluripotency markers in the MB (Figs. 6, 7(b) and 8). In contrast, downregulated BMP4 in the TW had no observable effect on mESC pluripotecny markers, thereby maintaining a low level of pluripotency markers expression (Figs. 7(b) and 8). Notably, BMP4 expression was significantly upregulated only in the MB culture compared to the 6-WP and TW cultures (Fig. 6). Enclosed micro-scale environment might have facilitated the upregulation of BMP4 in the MB. Because the cell growth behaviors in these cultures were the same (Fig. 4), amount of secreted factors in the culture environment would be approximately the same. However, in the MB,

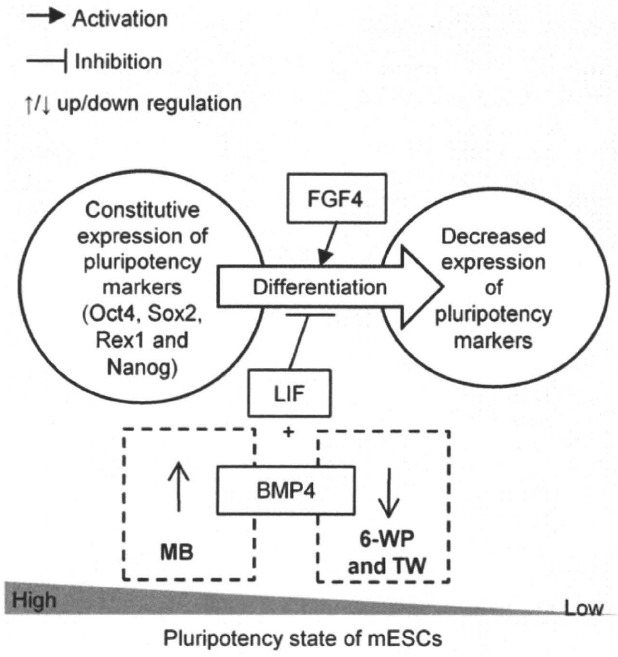

Fig. 8 A schematic diagram of the influence of soluble factors on the pluripotency markers in the embryonic stem cell culture environment. LIF and BMP4 cooperate to resist FGF4-induced differentiation. Effects of BMP4 on the pluripotency state of mESCs in the micro (MB) and macro-scale (TW) culture systems are also depicted

the culture volume was small (114 μL compared to the cell compartment volumes of 1.5 mL and 2 mL in the TW and 6-WP, respectively), and mass transfer was diffusion dominant due to small dimensions as well as the absence of a free interface between the culture medium and air (Yu et al. 2005). On the other hand, surface tension differences at the interface cause rapid convection in the macro-scale culture systems, and that creates a homogenous distribution of secreted soluble factors over the entire culture volume (Yu et al. 2005). Therefore, secreted soluble factors were accumulated and reached higher concentrations in the MB than in the 6-WP and TW. Moreover, they were presumably retained around the cell colonies at high concentrations for a longer time period in the MB owing to the diffusion dominant mass transfer. BMP4 can induce its own expression by a positive feedback mechanism (Vainio et al. 1993). Furthermore, owing to the relatively short half-life of BMP4, it is necessary to retain BMP4 near the cell for its activity (Miljkovic et al. 2008). Therefore, the higher exposure of cells to BMP4 in the MB culture than in the macro-scale cultures (the 6-WP and TW) may facilitate the feedback mechanism. This explains the observed upregulation and downregulation of BMP4 expression in the MB and macro-scale cultures, respectively (Fig. 6).

In spite of FGF4 accumulation, cells in the MB displayed a similar response in gene expression to that observed in the TW following FGF4 inhibition (Fig. 7(a)). However, inhibition of BMP4 activities resulted in significantly different effects in the MB and TW (Fig. 7(b)). Molecular diffusivities (inversely proportional to the cube root of molecular weight, MW) primarily determine the retention behavior of the soluble factors around the cells (Yu et al. 2005). FGF4 has a lower MW (22 kDa) than BMP4 (47 kDa), and may have diffused more quickly out of the cellular milieu. Therefore, it was unable to exert any influence on the cells as BMP4 did in the MB. In addition, extensively secreted FGF4 could have reached the threshold level of its activity equally in the MB and TW. These could be the plausible reason for the similar response observed in the TW and MB.

The average concentrations (total number of molecules divided by volume) of FGF4 and BMP4 in the MB might be the highest among the culture systems owing to the accumulation of these factors in the smallest volume. However, the cellular response to a soluble factor depends on the concentration level of the factor in the vicinity of the cell (local concentration). Both the average and local concentrations are influenced by various parameters of a soluble factor such as secretion, consumption, sequestration and release form the ECM. However, convection and diffusion only influence the local concentration. Owing to the diffusion dominant mass transfer in the MB, a soluble factor could be retained around the cells over time to reach a high concentration—all other parameters being the same in all culture systems. Therefore, in the MB, we could realize the combined effect of accumulation in a small volume and diffusion dominant mass transfer. However, we could not distinguish explicitly which concentration (average or local) reached the threshold level to impart a cellular response. To make the distinction, further investigation (experiments coupled with mathematical simulation) is necessary by taking the various parameters of a soluble factor into account along with diffusion and convection. This study, which characterizes the effects of soluble factors on ESC culture in the MB, provides a basis for the investigation.

mESCs secret FGF5, Nodal and BMP2 at low variable levels besides FGF4 and BMP4 (Wiles and Proetzel 2006). This micro-bioreactor and culture condition will be useful to study their effects in a diffusion dominant cellular environment, and will contribute to the understanding of ESC biology. The heterogeneity of ESCs during differentiation is one obstacle in obtaining lineage-specific cells useful for cell-based transplantation therapies (Singh and Terada 2007). Our micro-bioreactor can be used for obtaining relatively homogenous ESCs. In the absence of LIF, both FGF4 and BMP4 promote the differentiation of ESCs (Ying et al. 2003a). Therefore, the activity of soluble factors observed in the MB will provide an enhanced signaling microenvironment for controlling ESC differenti-

ation process in a monolayer format such as for neuronal (Ying et al. 2003b) or hepatocyte (Teratani et al. 2005) differentiation. By keeping the cellular environment in the upper chamber minimally disturbed, it is also possible to provide other soluble factors or inhibitors through the lower chamber to gain more precise control of the differentiation process.

5 Conclusions

In this study, we developed a membrane-based two-chambered micro-bioreactor for mESC culture to mimic the diffusion dominant mass transfer environment observed *in vivo*. The influence of soluble factors on cells in the micro-bioreator was compared with a macro-scale culture system. We observed enhanced retention of the pluripotent phenotype of mESCs in the micro-bioreactor owing to the enhanced effect of a soluble factor in a diffusion dominant microenvironment. A similar effect of the soluble factor was not observed in the macro-scale membrane-based Transwell insert culture system, in which soluble factors dissipated away from cell surrounding through inherent convection. This micro-bioreactor offers a suitable platform not only to understand the influence of secreted soluble factors on stem cell biology, but also to address an enhanced signaling environment to direct the ESC fate.

Acknowledgements M. M. Chowdhury was supported by Monbu-kagakusho scholarship from the Japan Ministry of Education, Culture, Sports, Science and Technology (MEXT). This research was supported in part by CREST from Japan Science and Technology Agency and GMSI (Global Center of Excellence for Mechanical Systems Innovation), The University of Tokyo. We would like to thank Dr. Masaki Nishikawa and Dr. Morgan Hamon for their useful suggestions regarding various technical aspects related to this study.

References

V.V. Abhyankar, G.N. Bittner, T.J. Kamp, D.J. Beebe, in 7th International Conference on Miniaturized Chemical and Biochemical Analysis Systems (Transducers Research Foundation, San Diego, California, USA, 2003), pp. 17–20.

E. Figallo, C. Cannizzaro, S. Gerecht, J.A. Burdick, R. Langer, N. Elvassore, G. Vunjak-Novakovic, Lab Chip **7**, 710–719 (2007)

P. Gadue, T.L. Huber, M.C. Nostro, S. Kattaman, G.M. Keller, Exp. Hematol. **33**, 955–964 (2005)

B.M. Johansson, M.V. Wiles, Mol. Cell. Biol. **15**, 141–151 (1995)

L. Kim, M.D. Vahey, H. Lee, J. Voldman, Lab Chip **6**, 394–406 (2006)

H. Kimura, T. Yamamoto, H. Sakai, Y. Sakai, T. Fujii, Lab Chip **8**, 741–746 (2008)

N. Korin, A. Bransky, U. Dinnar, S. Levenberg, Biomed. Microdev. **11**, 87–94 (2009)

T. Kunath, M.K. Saba-El-Leil, M. Almousailleakh, J. Wray, S. Meloche, A. Smith, Development **134**, 2895–2902 (2007)

D.A.F. Loebel, C.M. Watson, R.A.D. Young, P.P.L. Tam, Dev. Biol. **264**, 1–14 (2003)

S. Masui, S. Ohtsuka, R. Yagi, K. Takahashi, M.S. Ko, H. Niwa, BMC Dev. Biol. **8**, 45 (2008)

I. Meyvantsson, D.J. Beebe, Annu. Rev. Anal. Chem. **1**, 141–1427 (2008)

N.D. Miljkovic, G.M. Cooper, K.G. Marra, Osteoarthritis Cartilage **16**, 1121–1130 (2008)

M. Mohammadi, Science **276**, 955 (1997)

J.C. Mohr, J.J. de Pablo, S.P. Palecek, Biomaterials **27**, 6032–6042 (2006)

C.E. Murry, G. Keller, Cell **132**, 661–680 (2008)

A. Nagy, M. Gertsenstein, K. Vintersten, R. Behringer, *Manipulating the Mouse Embryo A Laboratory Manual*, 3rd edn. (Cold Spring Harbor, New York, 2003), pp. 32–38

H. Niwa, Development **134**, 635–646 (2007)

H. Niwa, J. Miyazaki, A.G. Smith, Nat. Genet. **24**, 372–376 (2000)

S. Ogawa, Y. Tagawa, A. Kamiyoshi, A. Suzuki, J. Nakayama, Y. Hashikura, S. Miyagawa, Stem Cells **23**, 903–913 (2005)

L. Palmqvist, C.H. Glover, L. Hsu, M. Lu, B. Bossen, J.M. Piret, R.K. Humphries, C.D. Helgason, Stem Cells **23**, 663–680 (2005)

J. M. Ruijter, C. Ramakers, W. M. H. Hoogaars, Y. Karlen, O. Bakker, M. J. B. van den Hoff, A. F. M. Moorman, Nucleic Acids Res. (2009) doi:10.1093/nar/gkp045

A.M. Singh, N. Terada, Trends Cardiovasc. Med. **17**, 96–101 (2007)

A.G. Smith, Annu. Rev. Cell Dev. Biol. **17**, 435–462 (2001)

W.C. Smith, R.M. Harland, Cell **70**, 829–840 (1992)

T. Teratani, H. Yamamoto, K. Aoyagi, H. Sasaki, A. Asari, G. Quinn, H. Sasaki, M. Terada, T. Ochiya, Hepatology **41**, 836–846 (2005)

S. Vainio, I. Karavanova, A. Jowett, I. Thesleff, Cell **75**, 45–58 (1993)

G.M. Walker, H.C. Zeringue, D.J. Beebe, Lab Chip **4**, 91–97 (2004)

M. V. Wiles, G. Proetzel, in *Embryonic Stem cells A Practical Approach*, ed. by E. Notarianni, M.J. Evans (Oxford University Press, New York, 2006), pp. 112–119

Q.L. Ying, J. Nichols, I. Chambers, A. Smith, Cell **115**, 281–292 (2003a)

Q.L. Ying, M. Stavridis, D. Griffiths, M. Li, A. Smith, Nat. Biotechnol. **21**, 183–186 (2003b)

Q.L. Ying, J. Wray, J. Nichols, L. Batlle-Morera, B. Doble, J. Woodgett, P. Cohen, A. Smith, Nature **453**, 519–524 (2008)

H. Yu, I. Meyvantsson, I.A. Shkel, D.J. Beebe, Lab Chip **5**, 1089–1095 (2005)

ARTICLE

BIOTECHNOLOGY and BIOENGINEERING

Production of a Non-Triple Helical Collagen α Chain in Transgenic Silkworms and Its Evaluation as a Gelatin Substitute for Cell Culture

Takahiro Adachi,[1,2] Xiaobiao Wang,[1] Tomoko Murata,[1] Masanobu Obara,[3] Hidenori Akutsu,[4] Masakazu Machida,[4] Akirihiro Umezawa,[4] Masahiro Tomita[1]

[1]Neosilk Co., Ltd., 3-13-26 Kagamiyama, Higashihiroshima, Hiroshima 739-0046, Japan; telephone: +81 82 431 0652; fax: +81 82 431 0654; e-mail: mtomita@neosilk.co.jp

[2]Hiroshima Prefectural Institute of Industrial Science and Technology, Higashihiroshima, Hiroshima, Japan

[3]Developmental Biology Laboratory, Department of Biological Science, Graduate School of Science, Hiroshima University, Higashihiroshima, Hiroshima, Japan

[4]National Center for Child Health and Development, Setagaya-ku, Tokyo, Japan

Received 16 December 2009; revision received 25 March 2010; accepted 29 March 2010

Published online 8 April 2010 in Wiley InterScience (www.interscience.wiley.com). DOI 10.1002/bit.22752

ABSTRACT: We generated transgenic silkworms that synthesized human type I collagen α1 chain [α1(I) chain] in the middle silk glands and secreted it into cocoons. The initial content of the recombinant α1(I) chain in the cocoons of the transgenic silkworms was 0.8%. The IE1 gene, a trans-activator from the baculovirus, was introduced into the transgenic silkworm to increase the content of the chain. We also generated silkworms homozygous for the transgenes. These manipulations increased the α1(I) chain content to 8.0% (4.24 mg per cocoon). The α1(I) chain was extracted and purified from the cocoons using a very simple method. The α1(I) chain contained no hydroxyprolines due to the absence of prolyl-hydroxylase activity in the silk glands. Circular dichroism analysis showed that the secondary structure of the α1(I) chain is similar to that of denatured type I collagen, demonstrating the absence of the triple helical structure. Human skin fibroblasts were seeded on the α1(I) chain-coated dishes. The cells attached and spread, although at decreased chain concentrations the spreading rate was lower than that of the collagen and gelatin. Cynomolgus monkey embryonic stem cells cultured on the α1(I) chain-coated dishes maintained an undifferentiated state after 30 passages, and their pluripotency was confirmed by teratoma formation in severe combined immunodeficient mice. These results show that the recombinant human α1(I) chain is a promising candidate biomaterial as a high-quality and safe gelatin substitute for cell culture.

Biotechnol. Bioeng. 2010;106: 860–870.

KEYWORDS: transgenic silkworm; cocoon; collagen; gelatin; cell culture

Correspondence to: M. Tomita

Introduction

Collagen, a protein with a triple helical structure composed of three α chains, is used as a biomaterial for a variety of medical and cosmetic applications (Lee et al., 2001; Miyata et al., 1992). Gelatin, the denatured and fragmented form of collagen, is applied in medicine as a material for oral drug delivery and parenteral formulations (Gill and Feinberg, 2001; Tabata and Ikada, 1998). These materials come mainly from animal sources, which carry a risk of pathogen contamination and can also cause allergic reactions (Bradley, 1993; Mullins et al., 1996). One promising approach to overcome such problems is to produce them by recombinant means using appropriate hosts. For example, collagens have been produced successfully using host cells possessing prolyl-hydroxylase activity, which is required for the formation of the triple helical structure (Berg and Prockop, 1973; Fichard et al., 1997; Geddis and Prockop, 1993). Collagens have also been produced in host cells that did not possess sufficient prolyl-hydroxylase activity for triple helix formation but were transfected with prolyl-hydroxylase genes (John et al., 1999; Lamberg et al., 1996; Merle et al., 2002; Vuorela et al., 1997). In contrast, cells lacking hydroxylase activity have been utilized as hosts for the synthesis of recombinant gelatins (Olsen et al., 2003; Werten et al., 1999).

We previously generated transgenic silkworms that synthesized a recombinant fusion protein containing the collagen sequence in their silk glands and secreted it into cocoons. Due to the absence of prolyl-hydroxylase activity in the glands, prolyl residues in the collagen sequence were not hydroxylated (Tomita et al., 2003, 2005). To produce

prolyl-hydroxylated protein, prolyl-hydroxylase genes were simultaneously introduced to the silkworms along with the recombinant protein gene. The resulting silkworms produced a protein containing a prolyl-hydroxylated collagen sequence in their cocoons (Adachi et al., 2006). While these studies demonstrated the possibility of mass production of recombinant collagens in transgenic silkworms, we recognized an important issue that needed to be addressed: given that the recombinant protein was incorporated into insoluble silk fibers, the protein could not be extracted without using strong chaotropic reagents.

Silk fibers are composed mainly of two types of protein: fibroin and sericin. The former comprises 70–80% of all silk proteins, constitutes the core of insoluble silk fibers, and is synthesized in the posterior silk glands (PSGs). Sericin, which accounts for 20–30% of silk proteins, refers to a group of hydrophilic glue proteins that surround the fibroin core and are synthesized in the middle silk glands (MSGs; Garel et al., 1997; Grzelak, 1995). The above-described recombinant fusion protein containing the collagen sequence was expressed in the PSGs, resulting in production of the recombinant protein into the insoluble fibroin core (Tomita et al., 2005). Recently, we also developed a sericin promoter-driven recombinant protein expression system, in which recombinant proteins are expressed in the MSGs and secreted into hydrophilic sericin layers of silk fibers. Green fluorescent protein (Tomita et al., 2007), human serum albumin (Ogawa et al., 2007), and mouse IgG (Iizuka et al., 2009) were successfully produced in cocoons. These proteins were extractable from cocoons by soaking them in mild neutral aqueous solutions such as phosphate-buffered saline (PBS) or Tris-buffered saline.

In this study, we generated transgenic silkworms that expressed the full-length triple helical region of the human type I collagen α1 chain [α1(I) chain] in the MSGs. Type I collagen is the most abundant fibril-forming collagen in the human body. A common form of type I collagen is a heterotrimer composed of two α1(I) chains and one α2(I) chain. It is also known that α1(I) chains are able to form a homotrimer in the absence of α2(I) chain (Nicholls et al., 1979). The recombinant α1(I) chain expressed in the MSGs was efficiently secreted into cocoons and was easily recoverable. Given that the silk glands had no prolyl-hydroxylase activity, the chains contained no hydroxyproline residues. In addition, the recombinant α1(I) chain expressed in this study lacks the telopeptide and propeptide promoting triple helix formation (Doege and Fessler, 1986; Olsen et al., 2001; Rosenbloom et al., 1976). Therefore, the α1(I) chains did not form the homotrimer with the triple helical structure, and their physio-chemical properties were similar to those of gelatin rather than collagen. We tested the possibility of using the recombinant α1(I) chain as a cell culture scaffold, and found that cells could be cultured on the chain as on marketed gelatin. As the recombinant α1(I) chain has uniform molecular weight and no risks of animal-derived pathogen contamination, the recombinant chain may be useful as a high-quality and safe substitute for marketed gelatin.

Materials and Methods

Experimental Animals

A strain of silkworm, pnd-w1, was obtained from the National Institute of Agrobiological Science (Tsukuba, Japan). Larvae were reared at 25°C on an artificial diet (Nosan Corporation, Yokohama, Japan).

Vector Construction for Transgenic Silkworms

The vector COL1A1/pMSG for transgenic silkworms was constructed using a full-length cDNA coding for the pro α1 chain of human type I procollagen (GenBank Accession No. Z74615) obtained by RT-PCR from human placenta total RNA (Clontech, Palo Alto, CA). The PCR-amplified product was cloned into the pCR4-TOPO vector (Invitrogen, Carlsbad, CA) using a TOPO cloning system (Invitrogen), which yielded pCR4COL1A1. To obtain the DNA fragment containing the baculovirus polyhedrin 5′-untranslated region (UTR; nt 140–189; GenBank Accession No. M30925; Iizuka et al., 2008), the signal sequence of human calreticulin (nt 109–159; GenBank Accession No. M84739), and the cDNA for the triple helical region of the α1(I) chain (nt 654–3695; Fig. 1A), PCR was performed using pCR4COL1A1 as a template. A set of primers, calSP/COL1A1-F (5′-ATGCTGCTATCCGTGCCGTTGCTGCTC-GGCCTCCTCGGCCTGGCCGTCGCCGGCCCCATGGGT-CCCTCT-3′) and *Nru*I/STP/COL1A1-R (5′-TCGCGATT-AGGGAGGACCAGGG-GGACC-3′), was used for the first PCR. A second PCR was performed using the product of the first PCR as a template and *Nru*I/Bm5UTR/calSP-F (5′-TCGCGAAAGTATTTTACTGTTTTCGTAACAGTTTT-GTAATAAAAAAACCTATAAATATGCTGCTATCCGTG-CCG-3′) and *Nru*I/STP/COL1A1-R as a primer set. The amplified product was cloned into the pCR4-TOPO vector to generate pCR4BmUTRcalSPCOL1A1. The DNA fragment was re-excised from pCR4BmUTRcalSPCOL1A1 by digestion with *Nru*I, and inserted between the *Bombyx mori* sericin 1 promoter and the fibroin light chain 3′-flanking sequence of pMSG1.1MG (Iizuka et al., 2009), giving rise to COL1A1/pMSG (Fig. 1B).

A vector carrying the gene of baculovirus trans-activator IE1 (Tomita et al., 2007) was prepared as follows. To obtain the DNA fragment consisting of the polyhedrin 5′-UTR and the IE1 gene, PCR was performed using pIE1 (Tomita et al., 2007) as a template. A set of primers, *Eco*RV/Bm5UTR/IE1-F (5′-GATATCAAGTATTTTACTGTTTTC-GTAACAGTTTTGTAATAAAAAAACCTATAAATATGA-CGCAAATTAATTTTAACGCGTCG-3′) and *Bgl*/IE1-R (5′-AGATCTTTAATTAAATTCAAATTTTTTATATTTACAA-TTTAG-3′), was used for the PCR. The amplified product

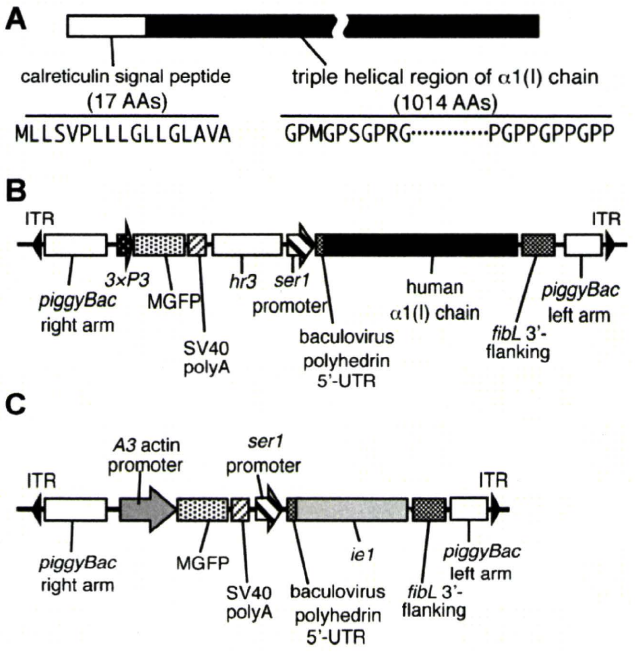

Figure 1. The structure of the transformation vector. **A**: The structure of the amino acid sequence of the α1(I) chain. The sequence of the α1(I) chain consists of a 17 amino acid (AA)-long calreticulin signal peptide (open box) and a 1,014 AA-long triple helical region of the α1(I) chain (filled box). **B**: The structure of the transformation vector COL1A1/pMSG. COL1A1/pMSG contained two expression units between the right and left arms of *piggyBac* as follows: *3xP3* promoter-driven MGFP cDNA with the SV40 polyA signal sequence (SV40 polyA) and the baculovirus-derived enhancer *hr3*-linked sericin 1 (*ser1*) promoter-driven α1(I) chain cDNA with the fibroin light chain gene polyA signal sequence (*fibL 3'*-flanking). ITR, inverted terminal repeat. **C**: Transformation vector pIM1. pIM1 contained two expression units between the right and left arms of *piggyBac* as follows: *Bombyx mori A3* actin promoter-driven MGFP cDNA with the SV40 polyA and *ser1* promoter-driven *ie1* gene with the *fibL* 3'-flanking.

was cloned into pCRII-TOPO vector (Invitrogen) to generate pCRBmUTRie1. The DNA fragment was released from pCRBmUTRie1 by digestion with *Eco*RV, and inserted between the *B. mori* sericin1 promoter and the fibroin light chain 3'-flanking sequence of pMSG1.1A3-MG, which had been created by replacing the *3xP3* promoter with the *B. mori A3* actin promoter (nt 1757–2595, GenBank Accession No. U49854) in pMSG1.1MG. The resulting vector was termed pIM1 (Fig. 1C).

Generation of Transgenic Silkworms

COL1A1/pMSG was injected with the helper vector pHA3PIG (Tamura et al., 2000) into pre-blastoderm embryos as described previously (Tomita et al., 2003). Hatched G_0 larvae were reared at 25°C to the moth stage. G_1 embryos obtained by sibling mating were screened for the expression of Monster Green Fluorescent Protein (MGFP; Promega, San Luis Obispo, CA) in the eyes and nervous tissues to obtain transgenic silkworms.

pIM1 was injected into eggs, and transgenic silkworms were created as described above, except that screening was performed by observing MGFP fluorescence in the larval body. The resulting transgenic silkworm (IM1) was crossed with silkworms carrying the α1(I) chain to obtain silkworms hemizygous for both the IE1 and the α1(I) chain genes.

To generate silkworms homozygous for the IE1 and the α1(I) chain genes, the above hemizygous silkworms were crossed with one another. From the next generations, homozygous silkworms for both genes were screened by genomic PCR using DNA extracted from blood cells as a template. Primers used in this PCR were designed from the genomic sequences flanking the transgene insertions, which were determined with an APA Transgene Locator Kit (BIO S&T Inc., Montreal, QC, Canada) according to the manufacturer's instructions.

SDS–PAGE and Western Blotting

Proteins in the sericin layer of silk fibers were extracted by incubating cocoons at 80°C for 5 min in a buffer consisting of 8 M urea, 2% 2-mercaptoethanol, and 50 mM Tris–HCl, pH 8.0. After centrifugation at 23,500*g* for 5 min, the obtained supernatant was electrophoresed on 0.1% SDS/5–20% polyacrylamide gradient gels (Atto, Tokyo, Japan) in running buffer (0.1% SDS, 12.5 mM Tris, and 125 mM glycine). The gels were stained with CBB-R250, and densitometric analyses were performed using the image-processing program, ImageJ (http://rsb.info.nih.gov/ij/). For Western blotting, the proteins on the gels were transferred onto PVDF membranes (Immobilon-P; Millipore, Billerica, MA), reacted with antihuman/bovine type I collagen antibodies (LB-1190; Cosmo Bio, Tokyo, Japan) and then with horseradish peroxidase (HRP)-linked anti-(rabbit IgG) antibodies (Cell Signaling Technology, Danvers, MA). The antigen–antibody complexes were visualized using the ECL Western Blotting Detection System (GE Healthcare, Little Chalfont, Buckinghamshire, UK).

Purification of the Recombinant α1(I) Chain From Transgenic Silkworm Cocoons

Cocoons were crushed into powder using a mill, suspended in a solution of 8 M urea and 0.5 M CH_3COOH, pH 2.0, at a concentration of 10 mg powdered cocoons/mL, and incubated at 4°C for 2 days with stirring. The resulting solution was filtered through filter paper and 70-μm nylon mesh. The solution was concentrated approximately threefold with an ultrafiltration membrane (Millipore) and urea was removed from the solution by adding 0.5 M CH_3COOH, pH 2.0, and subsequent ultrafiltration. NaCl was then added to the solution at a concentration of 0.5 M, and precipitated sericin was removed by centrifugation. Next, the recombinant α1(I) chain in the solution was collected by the addition of 3.5 M NaCl. The precipitate was

solubilized in 0.5 M CH_3COOH and subjected to dialysis against water.

N-Terminal Sequencing and Measurement of Amino Acid Composition

The N-terminal sequences of the purified α1(I) chain were determined with a G1000A protein sequencer (Hewlet Packard, Palo Alto, CA) using the standard protocol of Edman degradation. For the degradation reaction, 36 pmol of the chain were loaded onto the sequencer and the reaction was carried out for five cycles.

The purified α1(I) chain was hydrolyzed in 6 N HCl for 22 h at 110°C under vacuum, and analyzed for amino acid composition using a Hitachi 835 amino acid analyzer (Hitachi, Tokyo, Japan).

Determination of Melting and Gelation Points

The purified α1(I) chain was dissolved in distilled water at a concentration of 50 mg/mL, and the solution was subjected to determination of gelation and melting points as follows. The α1(I) chain solution was gradually cooled from 35 to −5°C at a rate of 1°C/min with a thermal cycler (Atto). The gelation point was determined by reading the temperature of the sample when its fluidity disappeared. For the analysis of the melting point, the α1(j) chain solution was incubated in icy water for 30 min to create a gel. The α1(I) chain gel was gradually heated from 0 to 40°C at a rate of 1°C/min with the thermal cycler. The melting point was determined by reading the temperature of the sample when the bubble at the bottom of the tube reached the surface of the sample solution.

Measurement of Circular Dichroism (CD) Spectra

CD spectra were recorded for the recombinant α1(I) chain using a spectropolarimeter J-820 (Jasco, Tokyo, Japan). The purified α1(I) chain was dissolved in 50 mM CH_3COOH at a concentration of 100 μg/mL for measurement in far ultraviolet (190–240 nm) regions, and the solution was placed in a cuvette with 2-mm pass length. The temperature was kept at 4°C during the procedures. Measurements were performed three times and the averaged values were plotted. Thermal transition curves were recorded by measuring molar ellipticity at 224 nm between 5 and 60°C at a rate of 30°C/h. The denaturing temperature was calculated with J-820 software (Jasco).

Endotoxin Test

An endotoxin level of the recombinant α1(I) chain was quantified using the limulus amebocyte lysate (LAL) as per the manufacturer's instructions (Endospecy ES-50M and Toxicolor DIA-MP; Seikagaku Biobusiness, Tokyo, Japan). Briefly, 50 μL standards or samples diluted with endotoxin-free water were mixed with LAL and incubated at 37°C for 30 min. After the substrate solution was added, the absorbance at 545 nm was measured. A standard curve was constructed by using the standards in the range of 0.02–0.1 EU/mL, and the concentration of endotoxin in each sample was determined by plotting the absorbance to the standard curve.

Quantifying the Spread of Human Dermal Skin Fibroblasts

The cell adhesivity to the recombinant α1(I) chain was analyzed by a quantitative cell-spreading assay using human dermal skin fibroblasts (HSFs; Kurabo, Osaka, Japan) as described previously (Yamada and Kennedy, 1984). In brief, a 96-well tissue culture plate (Becton Dickinson Labware, Franklin Lakes, NJ) was incubated with the recombinant α1(I) chain at various concentrations (0.31, 0.62, 1.25, 2.5, and 5.0 μg/mL) at 37°C for 1 h, treated with heat-denatured 0.5% bovine serum albumin to block the direct interaction between cells and the plate surface, and extensively washed with PBS. HSFs were seeded on the wells at a density of 1×10^4 cells per well, cultured in serum-free Dulbecco's modified Eagle's medium for 1 h, fixed in 4% paraformaldehyde, and viewed through a phase-contrast microscope (Nikon, Tokyo, Japan) to calculate the ratio of fully spreading cells to all cells observed in five randomly selected fields. HSFs were also cultured on the 96-well tissue culture plate coated with 10 μg/mL of the α1(I) chain as above to observe the cell morphology.

Culture of Cynomolgus Monkey Embryonic Stem (ES) Cells on Dishes Coated With the Recombinant α1(I) Chain

Cynomolgus monkey ES cells were cultured on murine embryonic fibroblast (MEF) feeder cells in Petri dishes (90 mm in diameter) according to previously established protocols (Cameron et al., 2006). Briefly, dishes were coated with the recombinant α1(I) chain by incubation with a solution of 1 mg/mL α1(I) chain for 30 min at room temperature. γ-Irradiated MEF cells were then cultured on the coated dishes as feeder cells for 1 day. Subsequently, monkey ES cells were seeded on MEF feeder layers and maintained by changing the medium. Immunostaining of monkey ES cell colonies was performed using NANOG, TRA1-81, SSEA-4, SOX2, and OCT4-specific primary antibodies (Millipore) according to the manufacturer's protocol. Nuclei were visualized by DAPI staining (Lin et al., 1976).

Monkey ES cells were injected subcutaneously into the hind leg of severe combined immunodeficient (SCID) mice (Suemori et al., 2001). Two months after injection, the mice were killed to remove teratomas. The teratomas

were then fixed with 4% paraformaldehyde in PBS, paraffin-embedded, sectioned, and histologically analyzed following staining with hematoxylin and eosin.

Results

Generation of Transgenic Silkworms

COL1A1/pMSG was injected into 9,834 pre-blastoderm embryos, and the hatched 5,282 G_0 larvae were allowed to develop to moths. G_1 embryos from the G_0 moths were screened for MGFP expression in the eyes and nervous tissues to obtain transgenic silkworms. Genomic Southern blot analysis of the transgenic silkworms demonstrated the existence of 41 independent transgenic lines with respect to the chromosomal insertion positions and copy numbers of the transgenes. Among them, 34 lines of transgenic silkworms with a single-copy transgene were selected, and the cocoon proteins of the lines were analyzed by SDS–PAGE. The line with the highest level of α1(I) chain expression was crossed with wild-type silkworms, and offspring hemizygous for the α1(I) chain gene were used in the following experiments as the COL249 line.

The worms of the COL249 line spun cocoons that were normal in appearance, size, and weight. Proteins in the sericin layer of the silk fibers of COL249 and wild-type silkworms were separated by SDS–PAGE and stained with CBB (Fig. 2, lanes 1–2). A band with an apparent molecular weight of 120 kDa was seen only in the cocoon proteins of COL249 (Fig. 2, lane 1). This band reacted with antihuman/bovine type I collagen antibody (Fig. 2, lane 6), indicating that this was the recombinant product from the human α1(I) chain gene. The band intensity of the recombinant α1(I) chain on the CBB-stained gel was quantified by densitometry. The content of the α1(I) chain was estimated to be 0.8% of the dried cocoon.

To increase the α1(I) chain content in the cocoon, a COL249 moth was crossed with an IM1 moth bearing the gene of the baculovirus-derived trans-activator IE1. Approximately 25% of the offspring carried both the α1(I) chain and IE1 genes hemizygously. The α1(I) chain/IE1 hemizygous silkworms (COL249/IM1) were further crossed with each other and silkworms homozygous for both the α1(I) chain and IE1 genes $(COL249/IM)^2$ were screened from the offspring by genomic PCR. Proteins in the cocoon extracts of COL249, COL249/IM, and $(COL249/IM)^2$ were separated by SDS–PAGE and stained with CBB (Fig. 3). By measuring the band intensity, the contents of the α1(I) chain in cocoons of the silkworm lines COL249, COL249/IM, and $(COL249/IM)^2$ were estimated to be 0.8%, 4.8%, and 8.0%, respectively. The average weights of cocoons in the COL249, COL249/IM, and $(COL249/IM)^2$ lines were 72, 65, and 53 mg, respectively. Although the cocoon weight decreased slightly with increased transgene copy numbers, the synthesis of the recombinant α1(I) chain per larvae was improved by this procedure; the amounts of the chain per cocoon of the COL249, COL249/IM, and $(COL249/IM)^2$ lines were 0.58, 3.12, and 4.24 mg, respectively.

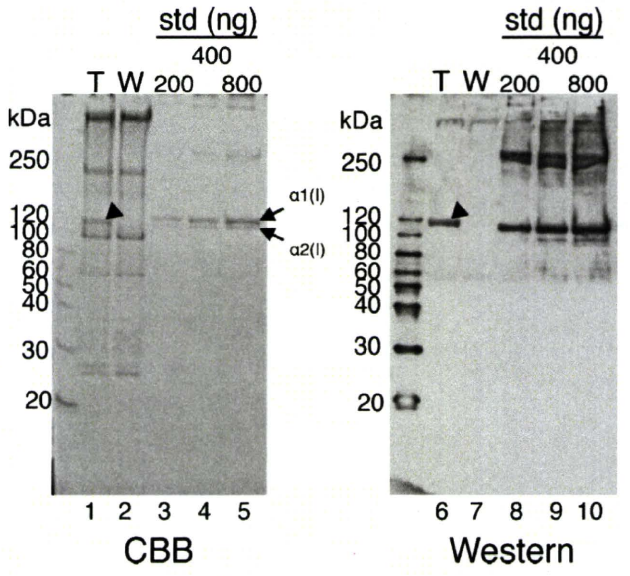

Figure 2. Expression of the α1(I) chain in cocoons of transgenic silkworms. The proteins in the cocoons of COL249 (T) and wild-type (W) silkworms were extracted with 8 M urea, 2% 2-mercaptoethanol, and 50 mM Tris–HCl, pH 8.0, separated by SDS–PAGE, and stained with CBB (**left panel**). Aliquots of the cocoon extracts were also assessed by Western blotting with antihuman/bovine type I collagen antibodies (**right panel**). Bovine pepsinized type I collagen in the amounts indicated was analyzed by CBB staining and Western blotting as a standard (std). The arrowheads in lanes 1 and 6 point to the band of the recombinant α1(I) chain. The arrows in lane 5 point to α1(I) and α2(I) chains of bovine type I collagen. Arabic numerals at the left side are molecular masses in kDa.

Extraction and Purification of the Recombinant α1(I) Chain From Cocoons

The extraction efficiency of the recombinant α1(I) chain from cocoons was examined. The powder of $(COL249/IM)^2$ cocoons was suspended in either PBS (Fig. 4A, lane 3), 0.5 M CH_3COOH, pH 3.0 (Fig. 4A, lane 4), 0.5 M CH_3COOH, pH 2.0 (Fig. 4A, lane 5), or 8 M urea and 0.5 M CH_3COOH, pH 2.0 (Fig. 4A, lane 6), at 4°C for 16 h, and the extracted proteins were analyzed by SDS–PAGE. Total proteins in the sericin layer of silk fibers of wild-type and transgenic silkworms were extracted by incubating cocoons at 80°C for 5 min in a buffer consisting of 8 M urea, 2% 2-mercaptoethanol, and 50 mM Tris–HCl, pH 8.0 (Fig. 4A, lanes 1 and 2). The ratios of the α1(I) chain extracted with the solutions to the total α1(I) chain in the sericin layer were calculated by quantifying the band intensities of the CBB-stained α1(I) chain. The efficiency of extraction was estimated to be 10% for PBS, 30% for 0.5 M CH_3COOH, pH 3.0, 50% for 0.5 M CH_3COOH, pH 2.0, and 80% for 8 M urea and 0.5 M CH_3COOH, pH 2.0. Thus, the use of CH_3COOH-solutions was more effective than PBS for extracting the recombinant α1(I) chain from

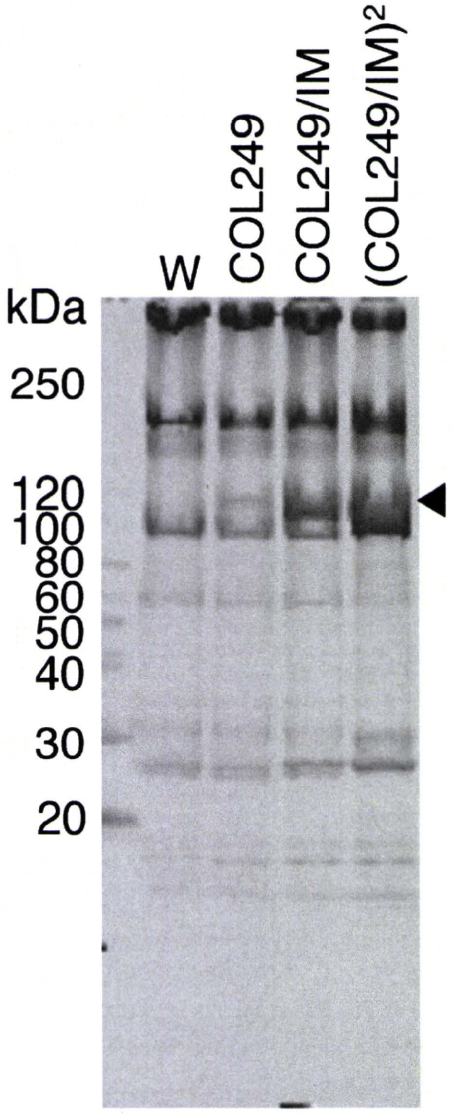

Figure 3. Increase in the α1(I) chain content in cocoons of transgenic silkworms. Transgenic silkworms were genetically modified to increase the amount of the α1(I) chain. Proteins were extracted from cocoons produced by wild-type (W), COL249, COL249/IM, and $(COL249/IM)^2$ silkworms, separated by SDS–PAGE, and stained with CBB. The arrowhead points to the band of the recombinant α1(I) chain. Arabic numerals at the left side are molecular masses in kDa.

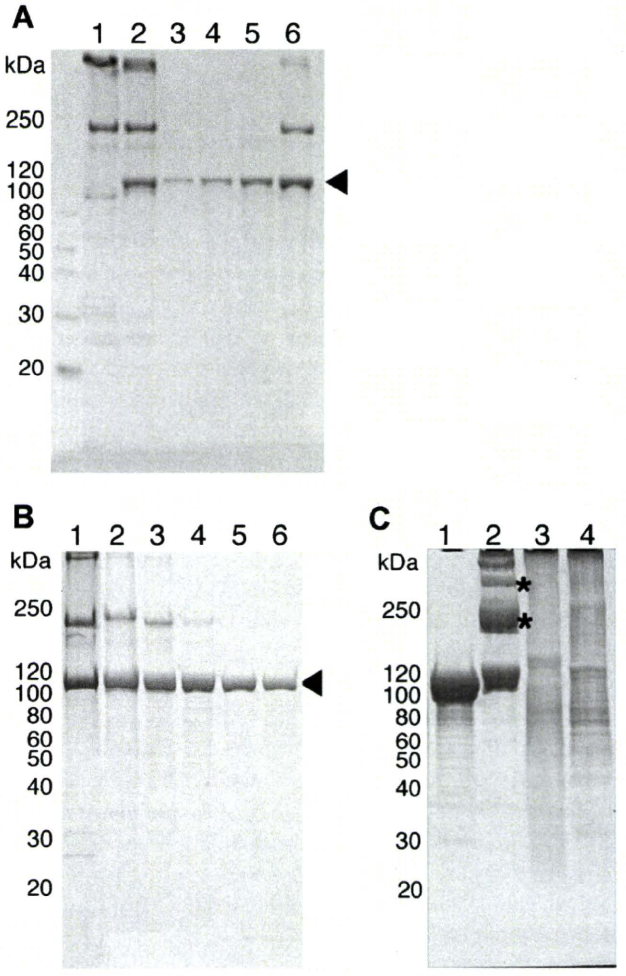

Figure 4. Extraction and purification of the α1(I) chain from cocoons of $(COL249/IM)^2$ silkworms. **A**: Extraction of the α1(I) chain from cocoons. Cocoon proteins were extracted with PBS (**lane 3**), 0.5 M CH_3COOH, pH 3.0 (**lane 4**), 0.5 M CH_3COOH, pH 2.0 (**lane 5**), and 8 M urea and 0.5 M CH_3COOH, pH 2.0 (**lane 6**). The extracted proteins were analyzed by SDS–PAGE. **Lanes 1** and **2** represent total proteins in the sericin layer of the silk fibers of wild-type and transgenic silkworms, respectively. The arrowhead points to the α1(I) chain. **B**: Analysis of the α1(I) chain in the purification processes. Cocoon proteins were extracted with 8 M urea and 0.5 M CH_3COOH, pH 2.0 (**lane 2**). The extracted proteins were concentrated by ultrafiltration (**lane 3**), and urea in the extract was removed by adding 0.5 M CH_3COOH, pH 2.0, and subsequent ultrafiltration (**lane 4**). After removing sericin by 0.5 M NaCl precipitation (**lane 5**), the α1(I) chain in the extract was collected by 4 M NaCl precipitation (**lane 6**). The proteins in each purification step were analyzed by SDS–PAGE and CBB staining. **Lane 1** represents total proteins in the sericin layer of the silk fibers. The arrowhead points to the α1(I) chain. **C**: Analysis of the purified α1(I) chain. Aliquots of 15 μg of proteins were electrophoresed and stained with CBB. **Lane 1**, the recombinant α1(I) chain; **lane 2**, bovine type I collagen; **lane 3**, alkaline-treated bovine gelatin; **lane 4**, acid-treated porcine gelatin. The asterisks in **lane 2** point to the dimer and trimer composed of the two and three α chains, respectively. Arabic numerals at the left side are molecular masses in kDa.

cocoons, and a major part of the α1(I) chain was extractive with 8 M urea and 0.5 M CH_3COOH, pH 2.0.

For purification of the α1(I) chain, 30 g of $(COL249/IM)^2$ cocoon powder, which was estimated to contain 2.4 g of the α1(I) chain, were suspended in 8 M urea and 0.5 M CH_3COOH, pH 2.0. The extracted α1(I) chain (Fig. 4B, lane 2) was concentrated by ultrafiltration (Fig. 4B, lane 3). The urea in the solution was removed by adding 0.5 M CH_3COOH, pH 2.0, and subsequent ultrafiltration. In this process, the endogenous sericin in the extract formed an insoluble aggregate, increasing the α1(I) chain content in the extract (Fig. 4B, lane 4). Small amounts of contaminated sericin were removed by 0.5 M NaCl precipitation (Fig. 4B, lane 5), and the α1(I) chain in the supernatant was then collected by precipitation with 4 M NaCl. The collected α1(I) chain was dissolved in 0.5 M CH_3COOH, pH 2.0, again, and the α1(I) chain solution was finally dialyzed against water (Fig. 4B, lane 6). The proteins in each

purification step and total proteins in the sericin layer (Fig. 4B, lane 1) were analyzed by SDS–PAGE, demonstrating that this simple purification process is sufficient to purify the α1(I) chain to apparent homogeneity. As a result, 990 mg of the α1(I) chain were purified from 30 g of cocoons; the recovery rate was estimated to be approximately 41%.

Biochemical Characterization

The purified recombinant α1(I) chain was analyzed by SDS–PAGE. Although small amounts of degradation products were found, the purified recombinant chain was composed of the polypeptide with a uniform molecular weight. The molecular weight of the chain was slightly smaller than the standard bovine α1(I) chain (Fig. 4C, lanes 1 and 2), indicating the possibility of insufficient prolyl-hydroxylation in the recombinant chain. The dimer (β chain) and trimer (γ chain) of the α chain, which were present in the standard collagen, were not detected from the purified recombinant chain, suggesting the absence of covalent cross-linking among the α1(I) chains. The molecular weight distribution of the recombinant α chain was quite different from that of the alkali-treated bovine (Fig. 4C, lane 3) or acid-treated porcine gelatins (Fig. 4C, lane 4). The gelatins gave broad molecular weight distributions because they were hydrolyzed products of collagens.

The α1(I) chain was subjected to an amino acid sequencer with five cycles of Edman degradation. The N-terminal amino acid sequencing of the α1(I) chain detected major and minor amino acid peaks in each cycle as shown in Table I. The sequence deduced from the minor peaks (GPM) was consistent with that of the predicted signal peptide cleavage (Fig. 1A) although peaks were not detected in the fourth and fifth cycles. The sequence from the major peaks (MGPSG) was probably derived from a cleavage at two amino acids downstream of the predicted site.

The amino acid composition of the purified α1(I) chain was determined after acid hydrolysis using a Hitachi L835 automated analyzer (Table II). The determined values were very similar to the predicted ones, except for the absence of hydroxyprolines and hydroxylysines.

The endotoxin levels of the α1(I) chain and the porcine gelatin were measured. The endotoxin level of the α1(I) chain was much lower (26 EU/g) than the gelatin (6,400 EU/g).

Structural Characterization

Far-ultraviolet (190–240 nm) CD spectra were recorded for the recombinant α1(I) chain, the native bovine type I collagen, the heat-denatured bovine type I collagen, and the porcine gelatin (Fig. 5A). The positive peak at 224 nm that is characteristic of the triple helical structure of collagen (Miller and Gay, 1982) was observed in the type I collagen. The gelatin exhibited a positive low peak at this wavelength, suggesting that the gelatin contained a partly formed triple helical structure in the molecule. In contrast, the recombinant α1(I) chain did not show a positive peak at 224 nm. The peak of the type I collagen disappeared when it was heat-denatured. The spectra of the denatured collagen were almost identical to those of the recombinant α1(I) chain. These results suggest that the α1(I) chain contained no triple helical structure. A negative peak at 198 nm represents the triple helical structure (Miller and Gay, 1982). The peak intensity at this wavelength of the recombinant α1(I) chain was similar to that of the heat-denatured collagen rather than that of gelatin, confirming the absence of the triple helical structure in the recombinant chain.

The 224-nm spectra were recorded for the recombinant chain, the native collagen, the denatured collagen and the gelatin at temperatures from 4 to 60°C (Fig. 5B). Apparent structural transition of the native collagen was observed in the range 39–46°C, which is in accordance with a report that the denatured temperature of bovine type I collagen is 42.8°C (Peltonen et al., 1980). In contrast, the recombinant α1(I) chain, the denatured collagen and the gelatin showed slight structural changes in the range 25–45°C.

The melting and gelation points of the 5% α1(I) chain or the gelatin solution were measured as described in the Materials and Methods Section. The melting and gelation

Table I. N-terminal sequencing.

Amino acid number	1	2	3	4	5
Major peaks	M	G	P	S	G
Minor peaks	G	P	M	—	—

Table II. Measurement of amino acid composition.

Amino Acid	Composition (mol%)	
	Recombinant α1(I) chain	Human α1(I) chain (predicted)
Aspartic acid	4.48	4.14
Threonine	1.56	1.58
Serine	2.91	3.35
Glutamic acid	7.71	7.30
Glycine	34.23	33.63
Alanine	11.72	11.74
Valine	1.81	1.87
Cystein	0.00	0.00
Methionine	0.33	0.69
Isoleucine	0.70	0.59
Leucine	2.12	1.87
Tyrosine	0.00	0.00
Phenylalanine	1.27	1.18
Hydroxylysine	0.00	2.37*
Lysine	3.66	1.18
Histidine	0.00	0.20
Arginine	4.71	5.03
Tryptophan	0.00	0.00
Hydroxyproline	0.00	11.44*
Proline	22.80	11.83
Total	100.00	100.00

*Assuming that all of lysine and proline residues in Y-position are hydroxylated.

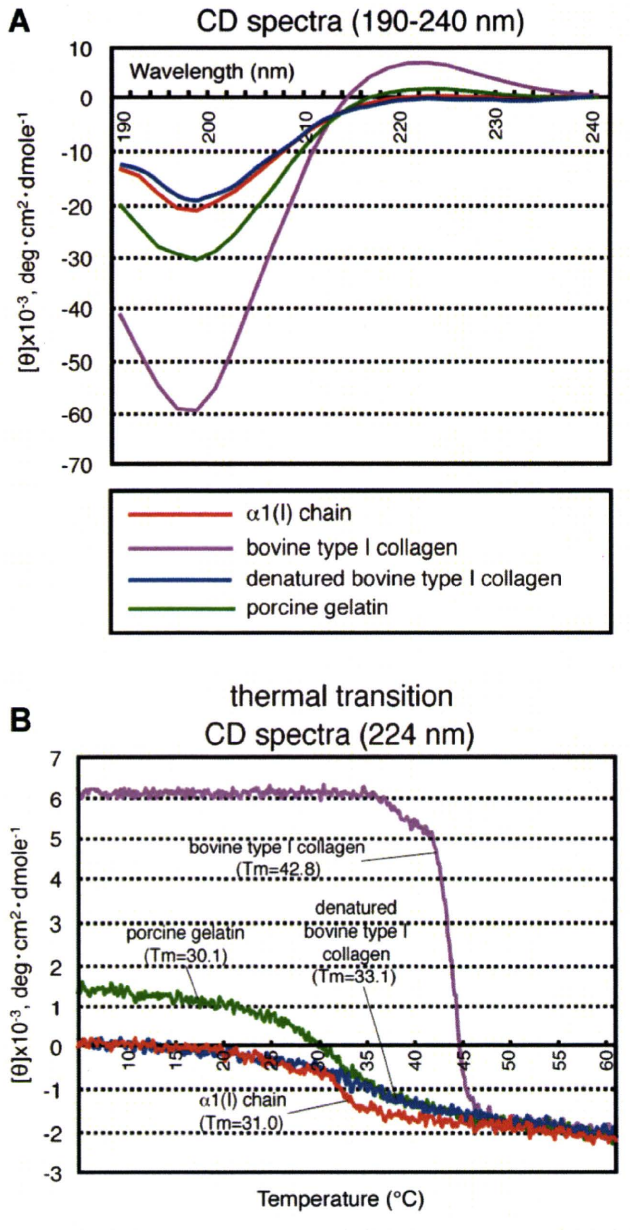

Figure 5. CD spectra of the α1(I) chain. **A:** Measurement of CD spectra of the α1(I) chain. Far-ultraviolet (190–240 nm) CD spectra were recorded for the recombinant α1(I) chain (red line), bovine type I collagen (pink line), denatured bovine type I collagen (blue line), and porcine gelatin (green line) at a concentration of 100 μg/mL. **B:** Thermal transition curves of the α1(I) chain. The CD spectra at 224 nm of the α1(I) chain, bovine type I collagen, denatured bovine type I collagen and porcine gelatin were monitored at temperatures from 4 to 60°C.

points of the α1(I) chain were 17 and 10°C, respectively, while the melting and gelation points of the gelatin were 30 and 26°C, respectively. Thus, both the melting and gelation points of the α1(I) chain were lower than the respective points of the gelatin, which may support the result from the measurement of CD spectra showing an absence of triple helical structures in the α1(I) chain. We also analyzed whether the α1(I) chain formed collagen fibrils under the physiological conditions as native collagen (Michalopoulos and Pitot, 1975) and found that the α1(I) chain did not form the fibrils (data not shown).

Cell Biological Properties

To investigate the cell biological properties of the recombinant α1(I) chain, HSFs were cultured on dishes coated with the α1(I) chain, the native collagen, or gelatin at various concentrations, and cell spreading on the materials was analyzed as described in the Materials and Methods Section (Fig. 6A). HSFs spread on all coating materials in a concentration-dependent manner. On collagen at concentrations of more than 0.63 μg/mL, HSFs spread at a rate of 100%. More than 80% of the cells spread on gelatin at concentrations >0.63 μg/mL, but 100% cell spreading was never observed even at the highest concentration tested (5.0 μg/mL). Cell spreading rates for the α1(I) chain at concentrations of <2.5 μg/mL were slightly low compared to those on gelatin at the same concentrations. However, HSFs spread on the α1(I) chain at a similar rate to on gelatin when inoculated at a concentration of 5.0 μg/mL. No differences were observed among cell morphologies when the cells were cultured on the α1(I) chain, the native collagen, or the gelatin at a concentration of 10 μg/mL (Fig. 6B, panels a–c). Cell-spreading was not observed on the uncoated dishes (Fig. 6B, panel d).

Cynomolgus monkey ES cells were cultured on feeder cells that had been cultured on dishes coated with the α1(I) chain or porcine gelatin. The ES cells cultured on dishes coated with the α1(I) chain formed tightly packed and flattened colonies (Fig. 7A, panel a). This morphology was the same as that of ES cell colonies cultured on dishes coated with porcine gelatin (Fig. 7A, panel b). Immunocytochemical studies confirmed that the monkey ES cell colonies on the α1(I) chain expressed the ES cell marker proteins NANOG, TRA1-81, SSEA-4, SOX2, and OCT4 (Fig. 7B). When the ES cells were subcutaneously injected into SCID mice after the passages on the α1(I) chain, the cells formed teratomas in the mouse tissues. Histological analyses of the teratomas showed formation of pigment epithelium, gastrointestinal epithelium, and cartilage (Fig. 7C). Thus, the α1(I) chain was confirmed to be useful for the maintenance of monkey ES cells.

Discussion

We generated transgenic silkworms that secreted the recombinant human α1(I) chain into the sericin layer of silk fibers. The content of the α1(I) chain in the cocoons of the established line COL249 was estimated to be 0.8%. By introducing the gene of the trans-activator IE1 into the silkworm as in our previous studies (Ogawa et al., 2007; Tomita et al., 2007), the expression of the α1(I) chain was enhanced to 4.8%. We then generated silkworms (COL249/

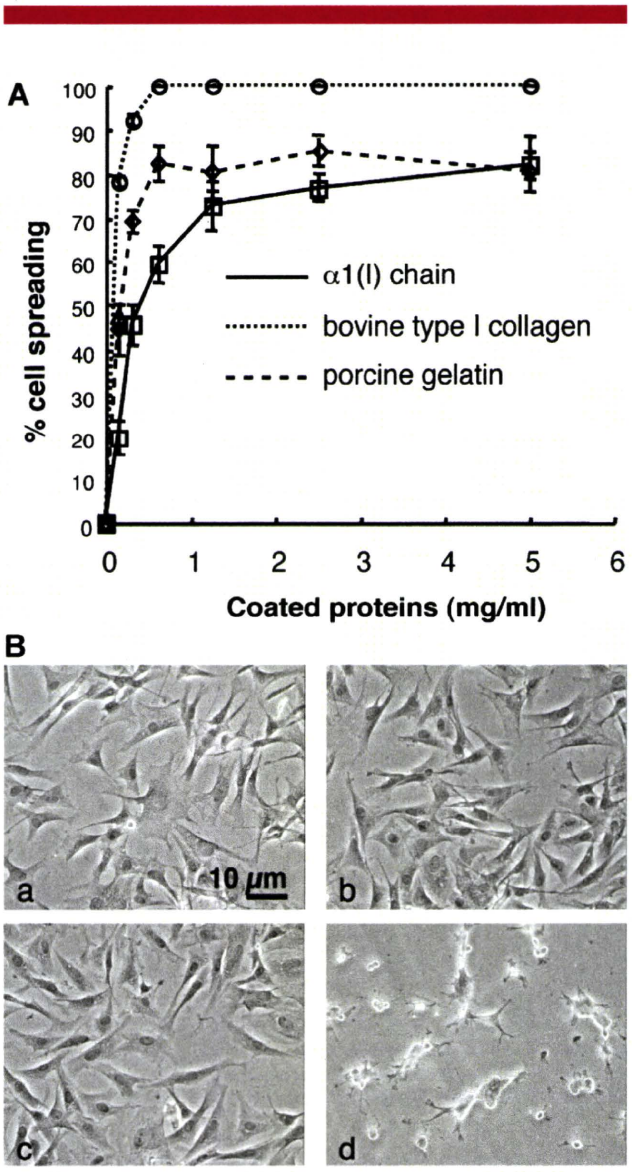

Figure 6. Spreading of HSFs on the α1(I) chain-coated dishes. **A**: Cell spreading assay using HSFs. The wells of tissue culture plates were coated with the α1(I) chain (black line), bovine type I collagen (dotted line), and porcine gelatin (dashed line) at various concentrations, and treated with heat-denatured bovine serum albumin to block the direct interaction between cells and the plate. HSFs were seeded on these wells and cultured for 1 h. The cells were then fixed, and the ratio of spreading cells to all cells in observed fields was calculated. **B**: Cell morphology of HSFs cultured on the α1(I) chain. HSFs were cultured on dishes coated with 10 μg/mL of the α1(I) chain (**a**), bovine type I collagen (**b**), porcine gelatin (**c**). The cells were also cultured on the uncoated but the albumin-treated dish (**d**). Scale bar, 10 μm.

IM)^2 homozygous for both the α1(I) chain and IE1 genes. This manipulation increased the α1(I) chain content up to 8.0%. Given that the average weight of a (COL249/IM)^2 cocoon was 53 mg, the α1(I) chain content per cocoon was calculated to be 4.24 mg. If 1,000 (COL249/IM)^2 silkworms were reared, we could produce 4.24 g of the α1(I) chain. The (COL249/IM1)^2 silkworm was generated from the pnd-w1 strain, which produces small cocoons (50–70 mg). Our preliminary experiment revealed that the cocoon weight could be increased to approximately 150 mg by crossing it with typical silkworm strains that produce 300- to 500-mg cocoons, leading to elevation of the α1(I) content to more than 10 mg per cocoon (data not shown). We also demonstrated the superiority of the transgenic silkworm system for the purification of the recombinant α1(I) chain. The α1(I) chain was highly purified from the cocoon extract by a simple method consisting of ultrafiltration and salt precipitation. Thus, this study offers experimental evidence for the viability of using transgenic silkworms in the production of the human recombinant α1(I) chain on an industrial scale.

Our previous study demonstrated that prolyl-hydroxylase activity is absent in silk glands (Adachi et al., 2005), and the recombinant fusion protein containing the collagen sequence expressed in the glands includes no hydroxyprolines (Tomita et al., 2005). The recombinant α1(I) chain produced in this study also contained no hydroxyprolines as predicted. The presence of hydroxyprolines is a prerequisite for forming the stable collagen triple helix (Berg and Prockop, 1973). In addition, the α1(I) chain did not contain the C-telopeptide and C-propeptide, which are known to promote triple helix formation (Doege and Fessler, 1986; Rosenbloom et al., 1976). Therefore, we postulated that the α1(I) chain is not capable of forming the triple helix. Indeed, CD spectra of the chain showed a complete absence of the triple helical structure. The importance of the telopeptide and propeptide for the triple helix formation was also shown in the previous studies. Unhydroxylated type I collagen with the telopeptide, and unhydroxylated α1(I) chain with the telopeptide and propeptide were synthesized as correctly folded triple helices in yeast (Olsen et al., 2001) and tobacco (Ruggiero et al., 2000), respectively. On the other hand, this study revealed that the animal-derived gelatin contained a partially folded triple helix, suggesting the significance of hydroxyprolines in the stability of triple helix. To further clarify the difference of physiological properties among the recombinant α1(I) chain, the gelatin and the collagen, we investigated the gelation and fibril-forming properties of the α1(I) chain. Unlike the collagen, the α1(I) chain did not form collagen fibrils under the physiological conditions examined. In contrast, the α1(I) chain, as well as the gelatin, gelated at lower temperatures than physiological ones. The melting and gelation points of the α1(I) chain were lower than those of gelatin. Thus, the physico-chemical properties of the recombinant α1(I) chain were similar to gelatin rather than collagen. However, due to the complete absence of the triple helical structure, the properties of the α1(I) chain differed slightly from those of gelatin.

The α1(I) chain promoted cell attachment and the spread of HSFs, but the cell-spreading rates for the α1(I) chain as well as gelatin were lower than those for collagen at all concentrations tested. At decreased concentrations of the materials, fewer cells spread on the α1(I) chain than on gelatin. Thus, HSFs were likely able to distinguish among these three materials. The cell–collagen interaction is mediated via integrins. Integrins α1β1 and α2β1 recognize collagens as collagen receptors (Hynes, 2002), and integrin

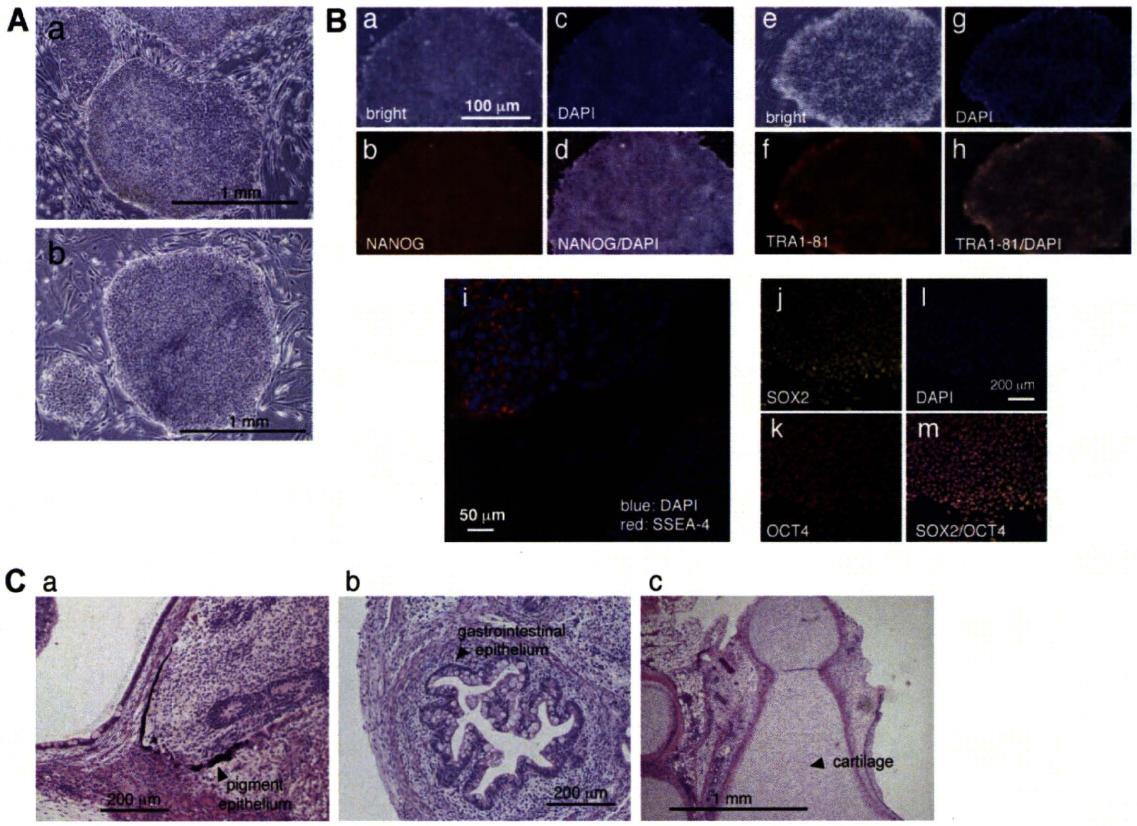

Figure 7. Culture of cynomolgus monkey ES cells on dishes coated with the α1(I) chain. **A**: Appearance of monkey ES cells. Cynomolgus monkey ES cells were cultured on feeder cells that had been cultured on dishes coated with the α1(I) chain (**a**) or porcine gelatin (**b**). Scale bar, 1 mm. **B**: Immunostain of the ES cell colonies. ES cell colonies were analyzed for the expression of marker proteins. **Panels (a–d** and **e–h)** show colonies immunostained with anti-NANOG and TRA1-81 antibodies, respectively. **Panels (a)** and **(e)**: appearances in bright fields; **panels (b)** and **(f)**: immunostained signals; **panels (c)** and **(g)**: DAPI-stained signals; **panels (d)** and **(h)**: mergers of immunostained and DAPI-stained signals. **Panel (i)** represents a colony stained with the anti-SSEA-4 antibody and DAPI. **Panels (j–m)** show a colony double-stained with anti-SOX2 and OCT4 antibodies. **Panel (j)**: immunostained signal with anti-SOX2 antibody; **panel (k)**: immunostained signal with anti-OCT4 antibody; **panel (l)**: DAPI-stained signal; **panel (m)**: merger of signals with anti-SOX2 and those with OCT4 antibodies. Scale bars, **(a)**: 100 μm; **(i)**: 50 μm; **(l)**: 200 μm. **C**: Teratoma formation in SCID mice. The ES cells were injected subcutaneously into the hind leg of SCID mice. Sections of the teratomas that formed were stained with hematoxylin and eosin. Arrowheads in **(a–c)** point to the pigment epithelium, gastrointestinal epithelium, and cartilage, respectively. Scale bars, **(a)** and **(b)**: 200 μm; **(c)**: 1 mm.

α5β1 indirectly recognizes it via collagen-bound fibronectin (Mould et al., 1997). Although the detailed mechanism is unknown, the complete absence of hydroxyprolines or the triple helical structure in the α1(I) chain may be responsible for this discrimination. At concentrations >5.0 μg/mL, however, HSFs spread on the α1(I) chain at a similar rate to that of gelatin. At a concentration of 10 μg/mL, the cell morphology was indistinguishable from that on collagen or gelatin. These results emphasize the practical utility of the recombinant α1(I) chain as a cell scaffold.

To demonstrate the practicality of the α1(I) chain, monkey ES cells were cultured on chain-coated dishes. After 30 passages, the monkey ES cell colonies maintained excellent morphology and the expression of several marker proteins for ES cells. The pluripotency of the cells was also confirmed by the formation of teratomas in SCID mice.

Gelatins are generally used for culturing ES or iPS cells. However, most marketed gelatins are derived from bovine or porcine bone, and therefore there is a risk of contamination with animal-derived pathogens, including viruses. In contrast, the recombinant α1(I) chain developed in this study does not pose such a risk because the chain is extracted from silk cocoons without using animal-derived materials. In addition, the α1(I) chain is composed of human sequences with constant molecular weight. Unlike the animal-derived gelatin extracted by hydrolyzing tissue collagens, the quality of the chain can be easily controlled with lot-to-lot consistency. The endotoxin level of the α1(I) chain was much lower than marketed gelatins. The recombinant α1(I) chain is a promising candidate material for use as a high-quality gelatin substitute for tissue engineering, drug delivery, and other applications.

References

Adachi T, Tomita M, Yoshizato K. 2005. Synthesis of prolyl 4-hydroxylase α subunit and type IV collagen in hemocytic granular cells of silkworm,

Bombyx mori: Involvement of type IV collagen in self-defense reaction and metamorphosis. Matrix Biol 24:136–154.

Adachi T, Tomita M, Shimizu K, Ogawa S, Yoshizato K. 2006. Generation of hybrid transgenic silkworms that express *Bombyx mori* prolyl-hydroxylase alpha-subunits and human collagens in posterior silk glands: Production of cocoons that contained collagens with hydroxylated proline residues. J Biotechnol 126:205–219.

Berg RA, Prockop DJ. 1973. The thermal transition of a non-hydroxylated form of collagen. Evidence for a role for hydroxyproline in stabilizing the triple-helix of collagen. Biochem Biophys Res Commun 52:115–120.

Bradley R. 1993. The research programme on transmissible spongiform encephalopathies in Britain with special reference to bovine spongiform encephalopathy. Dev Biol Stand 80:157–170.

Cameron CM, Hu WS, Kaufman DS. 2006. Improved development of human embryonic stem cell-derived embryoid bodies by stirred vessel cultivation. Biotechnol Bioeng 94:938–948.

Doege KJ, Fessler JH. 1986. Folding of carboxyl domain and assembly of procollagen I. J Biol Chem 261:8924–8935.

Fichard A, Tillet E, Delacoux F, Garron R, Ruggiero F. 1997. Human recombinant alpha1(V) collagen chain. Homotrimeric assembly and subsequent processing. J Biol Chem 272:30083–30087.

Garel A, Deleage G, Prudhomme JC. 1997. Structure and organization of the *Bombyx mori* sricin 1 gene and of the sericins 1 deduced from the sequence of the Ser 1B cDNA. Insect Biochem Mol Biol 27:469–477.

Geddis AE, Prockop DJ. 1993. Expression of human COL1A1 gene in stably transfected HT1080 cells: The production of a thermostable homotrimer of type I collagen in a recombinant system. Matrix 13:399–405.

Gill J, Feinberg J. 2001. Saquinavir soft gelatin capsule: A comparative safety review. Drug Saf 24:223–232.

Grzelak K. 1995. Control of expression of silk protein genes. Comp Biochem Physiol 110:671–681.

Hynes RO. 2002. Integrins: Bidirectional, allosteric signaling machines. Cell 110:673–687.

Iizuka M, Tomita M, Shimizu K, Kikuchi Y, Yoshizato K. 2008. Translational enhancement of recombinant protein synthesis in transgenic silkworms by a 5'-untranslated region of polyhedrin gene of *Bombyx mori* Nucleopolyhedrovirus. J Biosci Bioeng 105:595–603.

Iizuka M, Ogawa S, Takeuchi A, Nakakita S, Kubo Y, Miyawaki Y, Hirabayashi J, Tomita M. 2009. Production of a recombinant mouse monoclonal antibody in transgenic silkworm cocoons. FEBS J 276:5806–5820.

John DC, Watson R, Kind AJ, Scott AR, Kadler KE, Bulleid NJ. 1999. Expression of an engineered form of recombinant procollagen in mouse milk. Nat Biotechnol 17:385–389.

Lamberg A, Helaakoski T, Myllyharju J, Peltonen S, Notbohm H, Pihlajaniemi T, Kivirikko KI. 1996. Characterization of human type III collagen expressed in a baculovirus system. Production of a protein with a stable triple helix requires coexpression with the two types of recombinant prolyl 4-hydroxylase subunit. J Biol Chem 271:11988–11995.

Lee CH, Singla A, Lee Y. 2001. Biomedical applications of collagen. Int J Pharm 221:1–22.

Lin MS, Alfi OS, Donnell GN. 1976. Differential fluorescence of sister chromatids with 4'-6-diamidino-2-phenylindole. Can J Genet Cytol 18:545–547.

Merle C, Perret S, Lacour T, Jonval V, Hudaverdian S, Garrone R, Ruggiero F, Theisen M. 2002. Hydroxylated human homotrimeric collagen I in Agrobacterium tumefaciens-mediated transient expression and in transgenic tobacco plant. FEBS Lett 515:114–118.

Michalopoulos G, Pitot HC. 1975. Primary culture of parenchymal liver cells on collagen membranes. Morphological and biochemical observations. Exp Cell Res 94:70–78.

Miller EJ, Gay S. 1982. The collagens: An overview and update. Methods Enzymol 82:3–32.

Miyata T, Taira T, Noishiki Y. 1992. Collagen engineering for biomaterial use. Clin Mater 9:139–148.

Mould AP, Askari JA, Aota S, Yamada KM, Irie A, Takada Y, Mardon HJ, Humphries MJ. 1997. Defining the topology of integrin alpha5 beta1-fibronectin interactions using inhibitory anti-alpha5 and anti-beta1 monoclonal antibodies. Evidence that the synergy sequence of fibronectin is recognized by the amino-terminal repeats of the alpha5 subunit. J Biol Chem 272:17283–17292.

Mullins RJ, Richards C, Walker T. 1996. Allergic reactions to oral, surgical and topical bovine collagen. Anaphylactic risk for surgeons. Aust NZ J Ophthalmol 24:257–260.

Nicholls AC, Pope FM, Schloon H. 1979. Biochemical heterogeneity of osteogenesis imperfecta: New variant. Lancet 1:1193.

Ogawa S, Tomita M, Shimizu K, Yoshizato K. 2007. Generation of a transgenic silkworm that secretes recombinant proteins in the sericin layer of cocoon: Production of recombinant human serum albumin. J Biotechnol 128:531–544.

Olsen DR, Leigh SD, Chang R, McMullin H, Ong W, Tai E, Chisholm G, Birk DE, Berg RA, Hitzeman RA, Toman PD. 2001. Production of human type I collagen in yeast reveals unexpected new insights into the molecular assembly of collagen trimers. J Biol Chem 276:24038–24043.

Olsen D, Yang C, Bodo M, Chang R, Leigh S, Baez J, Carmichael D, Perala M, Hamalainen ER, Jarvinen M, Polarek J. 2003. Recombinant collagen and gelatin for drug delivery. Adv Drug Del Rev 55:1547–1567.

Peltonen L, Palotie A, Hayashi T, Prockop DJ. 1980. Thermal stability of type I and type III procollagens from normal human fibroblasts and from a patient with osteogenesis imperfecta. Proc Natl Acad Sci U S A 77:162–166.

Rosenbloom J, Endo R, Harsch M. 1976. Termination of procollagen chain synthesis by puromycin. Evidence that assembly and secretion require a COOH-terminal extension. J Biol Chem 251:2070–2076.

Ruggiero F, Exposito JY, Bournat P, Gruber V, Perret S, Comte J, Olagnier B, Garrone R, Theisen M. 2000. Triple helix assembly and processing of human collagen produced in transgenic tobacco plants. FEBS Lett 469:132–136.

Suemori H, Tada T, Torii R, Hosoi Y, Kobayashi K, Imahie H, Kondo Y, Iritani A, Nakatsuji N. 2001. Establishment of embryonic stem cell lines from cynomolgus monkey blastocysts produced by IVF or ICSI. Dev Dyn 222:273–279.

Tabata Y, Ikada Y. 1998. Protein release from gelatin matrices. Adv Drug Deliv Rev 31:287–301.

Tamura T, Thibert C, Royer C, Kanda T, Abraham E, Kamba M, Komoto N, Thomas JL, Mauchamp B, Chavancy G, Shirk P, Fraser M, Prudhomme JC, Couble P. 2000. Germline transformation of the silkworm *Bombyx mori* L. using a *piggyBac* transposon-derived vector. Nat Biotechnol 18:81–84.

Tomita M, Munetsuna T, Adachi T, Hino R, Hayashi M, Shimizu K, Nakamura N, Tamura T, Yoshizato K. 2003. Transgenic silkworms produce recombinant human type III procollagen in cocoons. Nat Biotechnol 21:52–56.

Tomita M, Shimizu K, Yoshizato K. 2005. Transgenic silkworms that weave recombinant human collagen in cocoons. In: Yoshizato K, editor. Transgenic silkworms: Eurekah Bioscience Collection. Georgetown: Landes Bioscience. chapter 2657.

Tomita M, Hino R, Ogawa S, Iizuka M, Adachi T, Shimizu K, Sotoshiro H, Yoshizato K. 2007. A germline transgenic silkworm that secretes recombinant proteins in the sericin layer of cocoon. Transgenic Res 16:449–465.

Vuorela A, Myllyharju J, Nissi R, Pihlajaniemi T, Kivirikko KI. 1997. Assembly of human prolyl 4-hydroxylase and type III collagen in the yeast *Pichia pastoris*: Formation of a stable enzyme tetramer requires coexpression with collagen and assembly of a stable collagen requires coexpression with prolyl 4-hydroxylase. EMBO J 16:6702–6712.

Werten MW, van den Bosch TJ, Wind RD, Mooibroek H, de Wolf FA. 1999. High-yield secretion of recombinant gelatins by *Pichia pastoris*. Yeast 15:1087–1096.

Yamada KM, Kennedy DW. 1984. Dualistic nature of adhesion protein function: Fibronectin and its biologically active peptide fragments can autoinhibit fibronectin function. J Cell Biol 99:29–36.

ARTICLES

Aberrant silencing of imprinted genes on chromosome 12qF1 in mouse induced pluripotent stem cells

Matthias Stadtfeld[1,2,3]*, Effie Apostolou[1,2,3]*, Hidenori Akutsu[4], Atsushi Fukuda[5], Patricia Follett[1], Sridaran Natesan[6], Tomohiro Kono[5], Toshi Shioda[2] & Konrad Hochedlinger[1,2,3]

Induced pluripotent stem cells (iPSCs) have been generated by enforced expression of defined sets of transcription factors in somatic cells. It remains controversial whether iPSCs are molecularly and functionally equivalent to blastocyst-derived embryonic stem (ES) cells. By comparing genetically identical mouse ES cells and iPSCs, we show here that their overall messenger RNA and microRNA expression patterns are indistinguishable with the exception of a few transcripts encoded within the imprinted *Dlk1–Dio3* gene cluster on chromosome 12qF1, which were aberrantly silenced in most of the iPSC clones. Consistent with a developmental role of the *Dlk1–Dio3* gene cluster, these iPSC clones contributed poorly to chimaeras and failed to support the development of entirely iPSC-derived animals ('all-iPSC mice'). In contrast, iPSC clones with normal expression of the *Dlk1–Dio3* cluster contributed to high-grade chimaeras and generated viable all-iPSC mice. Notably, treatment of an iPSC clone that had silenced *Dlk1–Dio3* with a histone deacetylase inhibitor reactivated the locus and rescued its ability to support full-term development of all-iPSC mice. Thus, the expression state of a single imprinted gene cluster seems to distinguish most murine iPSCs from ES cells and allows for the prospective identification of iPSC clones that have the full development potential of ES cells.

Induced pluripotent stem cells (iPSCs), generated by the overexpression of transcription factors such as Oct4 (also called Pou5f1), Sox2, Klf4 and c-Myc in somatic cells[1,2], have enormous therapeutic potential as they enable the derivation of patient-specific pluripotent cell lines to study and possibly treat degenerative diseases. Although the generation of iPSCs is technically simple and ethically uncontroversial, it remains unclear whether iPSCs are molecularly and functionally different from ES cells derived from blastocysts, which are considered the gold standard for pluripotent cells. Previously published reports indicate high similarities between ES cells and iPSCs, including indistinguishable global histone modification and DNA methylation patterns[3,4]. In addition, iPSCs, like ES cells, give rise to numerous differentiated cell types, including the germ line, in the context of chimaeric animals[5,6]. More recently, iPSCs have been shown to support the development of all-iPSC mice using tetraploid (4n) embryo complementation[7–9], the most stringent assay for developmental potential[10,11].

Despite these similarities, there is emerging evidence for substantial differences between ES cells and iPSCs. For example, most iPSC clones give rise to low-grade chimaeras after injection into diploid blastocysts and fail to support the development of postnatal all-iPSC mice upon 4n embryo complementation[12–14]. At the molecular level, major differences in mRNA and microRNA (miRNA) expression[15–17], as well as in DNA methylation[18–20], have been reported between ES cells and iPSCs. These observations indicate that factor-mediated reprogramming results in abnormalities in resultant iPSCs, which could impede their therapeutic utility. In contrast, nuclear-transfer-mediated reprogramming gives rise to nuclear transfer ES cells that are molecularly and functionality indistinguishable from ES cells derived from fertilized embryos[21,22], raising the possibility that nuclear transfer generates cells that are more completely reprogrammed than iPSCs.

A potential limitation of the aforementioned studies is that ES cells were compared with iPSCs of different genetic backgrounds and harbouring viral transgenes, which are known to affect gene expression patterns[21,23] and the functionality[1,6] of cells. We therefore revisited the question of whether ES cells and iPSCs are equivalent by comparing genetically matched cell lines.

Transcriptional comparison of ES cells and iPSCs

To circumvent the potentially confounding effects of genetic background and viral integrations on gene expression patterns and developmental potential, we used a novel transgenic reprogramming system to generate genetically matched mouse ES cells and iPSCs[24]. Briefly, a polycistronic cassette expressing Oct4, Klf4, Sox2 and c-Myc[25] (OKSM) under the control of a doxycycline-inducible promoter was inserted into the collagen type I α1 (*Col1a1*) locus of ES cells expressing the reverse tetracycline-dependent transactivator (rtTA) from the *ROSA26* promoter[26]. These collagen-OKSM ES cells were then used to generate mice from which different somatic cell types were isolated and induced with doxycycline to derive genetically matched iPSCs for molecular and functional comparisons (Fig. 1a, b).

[1]Howard Hughes Medical Institute at Massachusetts General Hospital, Center for Regenerative Medicine; Harvard Stem Cell Institute, 185 Cambridge Street, Boston, Massachusetts 02114, USA. [2]Massachusetts General Hospital Cancer Center and Harvard Medical School, 149 13th Street, Charlestown, Massachusetts 02129, USA. [3]Department of Stem Cell and Regenerative Biology, Harvard University and Harvard Medical School, 42 Church Street, Cambridge, Massachusetts 02138, USA. [4]Department of Reproductive Biology, National Institute for Child Health and Development, Tokyo 157-8535, Japan. [5]Department of BioScience, Tokyo University of Agriculture, Tokyo 156-8502, Japan. [6]Sanofi-Aventis, 270 Albany Street, Cambridge, Massachusetts 02139, USA.
*These authors contributed equally to this work.

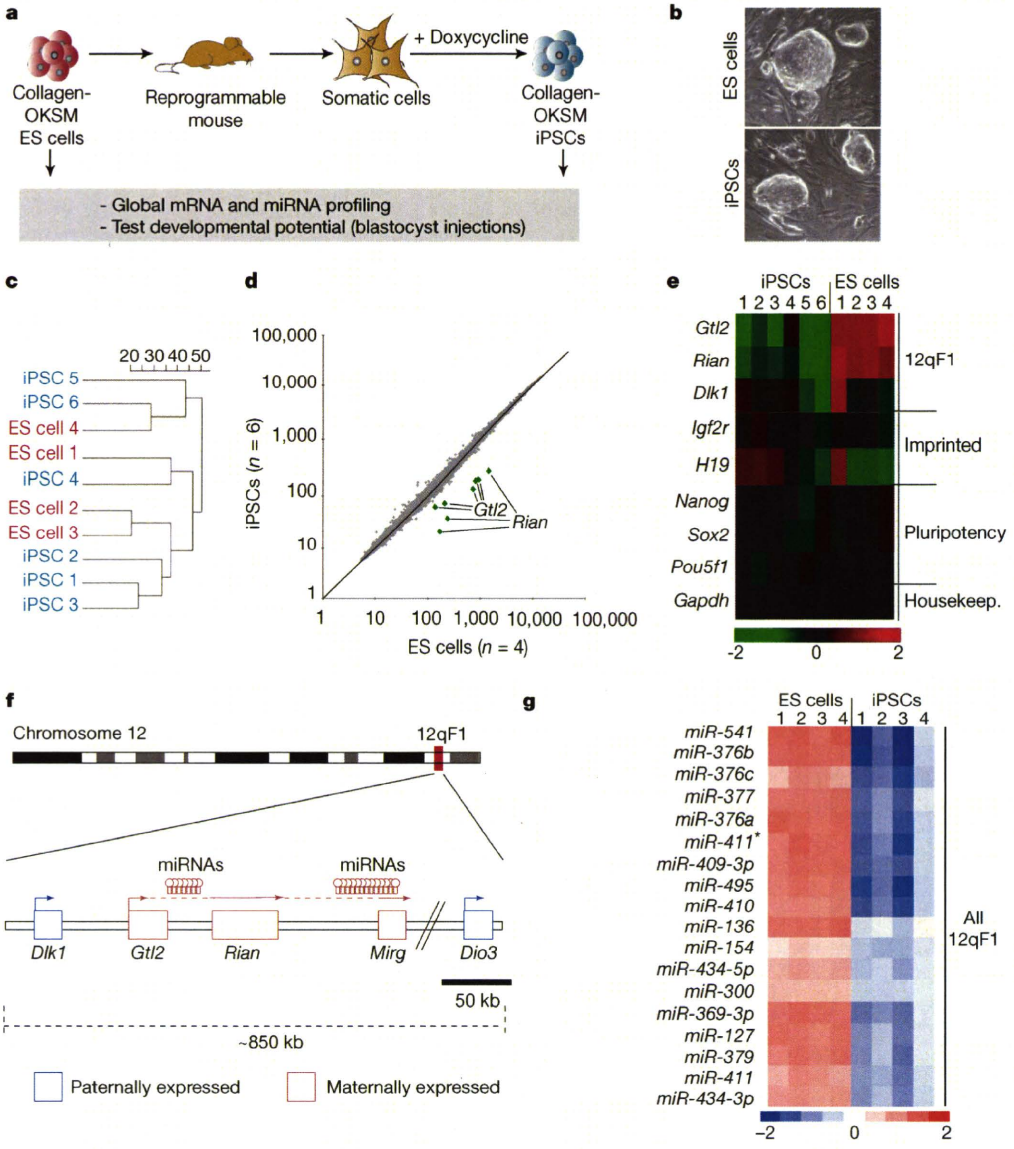

Figure 1 | Aberrant silencing of the *Dlk1–Dio3* gene cluster in mouse iPSCs. **a**, Strategy for comparing genetically matched ES cells and iPSCs generated with the doxycycline-controllable collagen-OKSM system. **b**, Morphology of collagen-OKSM ES cells and iPSCs. **c**, Unsupervised clustering of four ES cell and six derivative iPSC lines based on microarray expression data. **d**, Scatter plot of microarray data comparing iPSCs and ES cells with differentially expressed genes highlighted in green (twofold, $P < 0.05$, *t*-test with Benjamini–Hochberg correction). **e**, Heat map showing relative expression levels of selected mRNAs in ES cells and iPSCs. **f**, Schematic representation of the *Dlk1–Dio3* gene cluster with maternally and paternally expressed transcripts shown in red and blue, respectively. **g**, Heat map showing miRNAs that are differentially expressed between ES cells and iPSCs (twofold, $P < 0.01$, *t*-test).

We first compared the abilities of parental collagen-OKSM ES cells and iPSCs derived from mouse embryonic fibroblasts (MEFs) to support the development of all-iPSC mice using 4n embryo complementation. The two tested ES cell lines gave rise to viable mice at expected frequencies (13–20%)[11], demonstrating that the OKSM transgene per se does not adversely affect development (Supplementary Table 1). In contrast, all four tested iPSC lines repeatedly failed to support the development of all-iPSC mice, indicating qualitative differences between these iPSCs and ES cells (Supplementary Table 1).

We reasoned that a transcriptional comparison of the iPSC lines that failed 4n complementation with matched 4n-complementation-competent ES cell lines might reveal molecular changes that explain the developmental deficits of iPSCs. Global mRNA profiling showed marked similarities in the overall transcriptional patterns of four collagen-OKSM ES cells and six derivative iPSCs and did not separate these cell lines using unsupervised clustering or principal component analysis (Fig. 1c and data not shown). In fact, only two transcripts were identified as differentially expressed (>2-fold difference, *t*-test, $P < 0.05$) between ES cells and iPSCs. These were the non-coding RNA *Gtl2* (also know as *Meg3*) and the small nucleolar RNA *Rian* (Fig. 1d, e).

Repression of *Dlk1–Dio3* transcripts in iPSCs

Gtl2 and *Rian* localize to the imprinted *Dlk1–Dio3* gene cluster on mouse chromosome 12qF1 and are maternally expressed in mammals (Fig. 1f)[27]. Both genes were strongly repressed in iPSC clones compared to ES cell clones, whereas expression of pluripotency and housekeeping genes remained unaffected (Fig. 1e). Quantitative PCR (qPCR) analysis of *Gtl2*, *Rian* and *Mirg*, another maternally expressed imprinted gene in the *Dlk1–Dio3* cluster, confirmed transcriptional silencing in iPSCs (Supplementary Fig. 1a). Expression of other imprinted genes showed clone-to-clone variations, as was previously seen for ES cells[28], but no consistent differences between ES cells and iPSCs (Fig. 1e and Supplementary Table 2). This shows that imprinted gene silencing is not a genome-wide phenomenon. Of note, we failed to detect differences with the collagen-OKSM system